ABSTRACT

HUGHES, DAVID BURGESS. An On-Site Performance Analysis of Residential Geothermal Heat Pumps. (Under the direction of Dr. Stephen Terry.)

The purpose of this study was to assess the on-site performance of geothermal heat pumps for residential heating and cooling. Two geothermal systems were selected for the study: one open groundwater system and one open groundwater/surface-water hybrid system. The systems are referred to as System A and System B respectively. System A uses groundwater from an abandoned well. System B uses a pond heat exchanger in series with the groundwater from a well. The groundwater travels through the pond heat exchanger to achieve additional heat transfer, as the initial groundwater setup did not seem sufficient when the system was first operated.

System A is located outside of Durham, NC and System B is located outside of Hillsborough, NC. Both were installed to replace existing conventional air-to-air systems. For comparison purposes, a conventional air-source heat pump was monitored as well. This system is referred to as System C and is located outside of Garner, NC. Because of complications with this data, the geothermal heat pump manufacturer's data was used as a primary comparison.

System A performed at 82% of the manufacturer's claimed efficiency while operating as a heat pump. System B reached 89% of manufacturer's claimed efficiency in the heating mode. Comparisons in the cooling mode varied largely depending on the calculations used. The different values are presented, but a specific comparison was not made.

An On-Site Performance Analysis of Residential Geothermal Heat Pumps

by
David Burgess Hughes

A thesis submitted to the Graduate Faculty of
North Carolina State University
in partial fulfillment of the
requirements for the degree of
Master of Science

Mechanical Engineering

Raleigh, North Carolina

2010

APPROVED BY:

_____	_____
Dr. Herbert Eckerlin	Dr. Jay Cheng

_____
Dr. Stephen Terry
Committee Chair

DEDICATION

This work is dedicated to my family, friends, and fiancé. I never could have accomplished this without them.

BIOGRAPHY

David Hughes was raised in Chapel Hill, North Carolina. He was fortunate in his youth to have had supportive, caring, hard-working, and principled family and friends. His youth is remembered fondly.

After high school, David left the Piedmont to attend UNC-Asheville in the mountains of western North Carolina. There he studied hard, worked many interesting jobs, and met the girl of his dreams. Somehow, after nearly five years of courting her, David convinced her to marry him.

Following graduation from NC State University David will work in energy service contracting, trying to create environmentally and economically sustainable solutions for today's energy engineering challenges.

TABLE OF CONTENTS

LIST OF FIGURES

LIST OF TABLES

1 Introduction

How we use energy is of critical importance to many vital aspects of our lives: our economy, environment, health, national security, and limited natural resources. Progress is being made towards development of technologies which reduce the negative impacts of many conventional energy systems. It is my belief that this reduction is most effectively achieved through energy conservation. While renewable energy systems are incredibly well-suited for some objectives, they are frequently more expensive than comparable energy conservation measures.

Geothermal heat pumps are often mistakenly categorized as a "renewable technology". In fact, these heat pumps are in many ways similar to conventional heat pumps, but with much higher efficiency. The efficiency of these systems is largely a function of design and installation parameters. This study investigates the performance of two geothermal heat pumps in comparison to the performance claimed by the heat pump manufacturer.

2 Geothermal Energy

2.1 Development

The Oxford English Dictionary defines *geothermal* as

> **geo thermal:** *a.*, of or pertaining to the internal heat of the earth (OED, 1989).

This internal heat of the earth has been used for more than 10,000 years in North America. Indigenous cultures have taken advantage of most every known hot spring in this country, using this natural source of heat for cooking, bathing, and refuge (DOE, 2006).

Since these earlier times, engineers have advanced methods of harnessing geothermal energy to where it is used in mineral extraction, power production, space conditioning, and countless other processes. In one of the most notable examples of geothermal energy use, the development of this natural resource followed in exactly that order. The ancient community of Montecerboli, in Tuscany, Italy, has used geothermal resources dating back to the Roman Empire. The mineral-rich waters which flowed from hot springs in the area were used in Roman bath houses. Sulfur, vitriol, alum, and boric acid were extracted from these waters and sold throughout Europe dating back to the 11th century (Lund, 2004). This community became later known as Larderello, after a Frenchman Francois de Larderel began using the high temperature geothermal steam in his boron extraction process in 1827. This led to extensive use of geothermal-steam turbines to provide mechanical work in the extraction of minerals. The abundance of "free" mechanical work attracted attention and in 1904

geothermal steam was used to produce electricity for the first time (Banks, 2008). Seven years later the Valle del Diavolo (Devil's Valley) power plant was constructed. The plant was producing 250 kW by 1913.

2.2 Thermogeology

The field of geothermal energy has expanded beyond these high temperature uses to include what British hydrogeologist David Banks calls thermogeology. He defines this specialty within the geothermal energy sector as:

"*the study of the occurrence, movement, and exploitation of low-enthalpy heat in the relatively shallow geosphere.*"(Banks, 2008)

The qualifier "low-enthalpy" refers to temperatures less than 30°C (86°F). The "relatively shallow geosphere" suggests depths of no more than 200 meters (656 ft). This defines the realm of all the geothermal energy which would be used in a typical geothermal heat pump. As will be explained, the large mass and relatively constant temperature of the shallow geosphere provides a heat reservoir, both sink and source, which is theoretically more efficient for use in heat pumps.

The effectiveness of using this thermal reservoir below our feet, as well as the specific methods for doing so, are explored and detailed in this study.

3 Heat Pumps

3.1 Background

Heating has historically been inexpensive through the combustion of low cost fuels. Heat pumps developed not for heating, but rather for refrigeration. A refrigeration unit "pumps" heat out of the enclosure which is being cooled. The first example of this dates back to 1755, when ice was first made mechanically by the Scotsman William Cullen, a professor at the University of Glasgow. Cullen used low pressure to boil ethyl ether (Dincer, 2003). This was strictly an academic pursuit and remained such for nearly eight decades.

By 1834 the first vapor-compression refrigerator had been designed and constructed by the American printer Jacob Perkins. Perkins received the first patent on a vapor-compression cooling machine. While his machine worked, Perkins likely did not understand many of the theoretical underpinnings of his invention (Radermacher & Hwang, 2005).

In 1852, another professor from Glasgow, Professor Thomson (known as Lord Kelvin nearly 40 years later), created the first theoretical explanation of mechanical cooling using an open heat pump system and described it in great detail, complete with compressor, expander, heat exchangers, and refrigerant (air). This open system transformed in Thomson's mind into a closed system much like the standard vapor-compression cycle used today (Heap, 1979).

By the late 19th century, other refrigeration methods had been developed and were commercially available, slowing the need for heat pump technology (Heap, 1979). The late 1920's and early 1930's saw the first large-scale commercialization of heat pumps. This was

soon followed by the installation of heat pumps in the residential market in the 1940's. By the early 1980's over one-million heat pumps had been installed as residential units (Brodowicz & Dyakowski, 1993).

3.2 Mechanics

By the 2nd Law of Thermodynamics, it is well understood that heat flows from hot to cold. Our experience tells us the same. Heat is released from a hot pot of water to the cooler surrounding air. The water will never become hotter spontaneously by absorbing heat from the cooler surrounding air.

A heat pump is a device which operates against this natural flow by "pumping" heat from cold to hot. Using an external power source, typically in the form of electrical power, heat can be gathered from a low-temperature source and concentrated to create a higher-temperature source. This is typically accomplished using a vapor-compression cycle[i]. The following diagram shows a simplified vapor-compression cycle (Cengel & Boles, 2008).

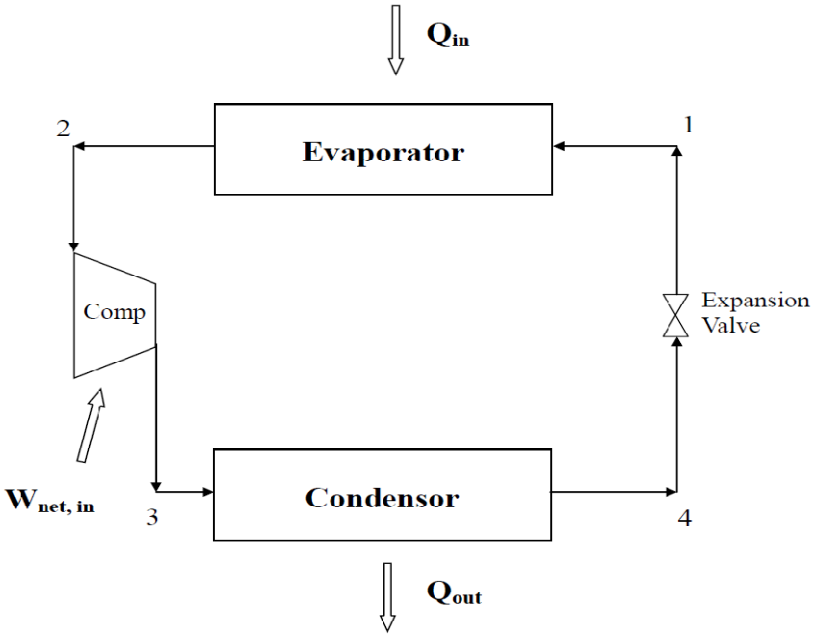

Figure 1. Vapor-Compression Cycle

The evaporator and the condenser are both heat exchangers. The evaporator is at a lower temperature (T_{low}) than the condenser temperature (T_{high}). The working fluid which absorbs heat at the evaporator, and thereby rejects heat at the condenser, is known as the refrigerant. Refrigerants are chosen based on several criteria with their thermodynamic properties being most significant in the operation of the heat pump[ii]. Refrigerants which boil and condense at temperatures T_{high} and T_{low} respectively are required for effective heat pump operation (Radermacher & Hwang, 2005).

Following the cycle from point 1 on the figure, saturated-liquid refrigerant at low pressure flows into the evaporator. Inside the evaporator the saturated liquid boils at T_{low}. The evaporation process is endothermic, drawing in a heat flow Q_{in}. This saturated vapor, at

point 2, then flows to the inlet of the compressor. Using work from an external source,$W_{net,in}$, the compressor compresses the saturated vapor, raising the pressure. The high-pressure superheated vapor, at point 3, then enters the condenser. The thermodynamic properties of this refrigerant are such that when the pressure is increased, fluid condenses at a higher temperature T_{high}. The superheated vapor condenses in the condenser. The condensation process is exothermic, releasing a heat flow Q_{out}. This high-pressure saturated liquid leaves the condenser and, at point 4, flows into the expansion valve. Here the pressure is reduced and the low-pressure saturated vapor completes the cycle before reentering the evaporator.

3.3 Ideal Heat Pumps

The ideal vapor-compression cycle, also known as the reversed Carnot cycle, is one in which each of the four processes described above occurs reversibly. Reversibility essentially implies that there are no losses, with respect to energy, in the system. This requires the compression to be isentropic and the evaporation and condensation to be isobaric. Such systems do not exist in reality. However, this ideal cycle is useful in determining the theoretical maximum efficiency in operating a heat pump with condenser and evaporator temperatures of T_{high} and T_{low} respectively.[iii]

Heat pump efficiency is measured in several different ways. Commercially, efficiencies are often measured in kW/ton, EER, SEER, or COP. These are discussed in more detail later. Academically, efficiencies are usually measured as a coefficient of performance, or COP. The COP of a heat pump is defined as

$$COP = \frac{desired\ output}{required\ input}$$

More specifically, the COP of a heat pump in the refrigeration cycle, COP_R, is

$$COP_R = \frac{Q_{in}}{W_{net,in}}$$

Where,

$$Q_{in} = Heat\ absorbed\ by\ the\ evaporator$$

$$W_{net,in} = Net\ electrical\ work\ input$$

The COP of a heat pump in the heating cycle, COP_{HP}, is

$$COP_{HP} = \frac{Q_{out}}{W_{net,in}}$$

Where,

$$Q_{out} = Heat\ rejected\ from\ the\ condensor$$

By the 1st Law of Thermodynamics, it is known that energy cannot be created nor destroyed. For the cycle in Figure 1 operating at steady state, this implies

$$Q_{out} = W_{net,in} + Q_{in}$$

Or,

$$W_{net,in} = Q_{out} - Q_{in}$$

By substituting the above equation into the equation for both COPs we see that

$$COP_R = \frac{Q_{in}}{Q_{out} - Q_{in}} = \frac{1}{\frac{Q_{out}}{Q_{in}} - 1}$$

And,

$$COP_{HP} = \frac{Q_{out}}{Q_{out} - Q_{in}} = \frac{1}{1 - \frac{Q_{in}}{Q_{out}}}$$

By the 2nd Law of Thermodynamics, along with the thermodynamic, or absolute, temperature scale, it can be shown that replacing the ratio of heat-transfer rates with the ratio of thermodynamic temperatures gives the COP of an ideal heat pump (Cengel & Boles, 2008). Therefore, the ideal coefficient of performance for a refrigerator and a heat pump, $COP_{r\text{-}ideal}$ and $COP_{hp\text{-}ideal}$, can be calculated as

$$COP_{r-ideal} = \frac{1}{\frac{T_{high}}{T_{low}} - 1}$$

And,

$$COP_{hp-ideal} = \frac{1}{1 - \frac{T_{low}}{T_{high}}}$$

By this, it can be seen mathematically that as the condenser temperature, T_{high}, approaches the evaporator temperature, T_{low}, the COP approaches infinity. This theoretical limit is the point at which the heat pump would no longer be required. If the evaporator temperature ever became higher than the condenser temperature the heat would "pump" itself by simply cooling off, just as our hot pot of water would in a cool room.

3.4 Real Heat Pumps

Since no process can actually occur in a thermodynamically irreversible manner, there will be associated inefficiencies with non-ideal heat pumps. These losses result from mainly from frictional losses in the working fluids, heat transfer losses to and from the surroundings, and inefficiencies in the compressor. A real heat pump will always have a lower coefficient of performance than the ideal heat pump acting between the same two heat reservoirs.

3.5 Conventional Heat Pumps

Most heat pumps in residential settings are air-to-air heat pumps. This means that heat is pumped from the outside air to the inside air in the winter and vice versa in the summer. Residential heat pumps are typically "split" systems. This refers to the arrangement of the heat pump components; the compressor and one heat exchanger are located outside the house while the expansion valve and the other heat exchanger are located inside. These systems are air-source heating and air-cooled cooling.

Efficiencies in conventional heat pumps are typically measured as EER or SEER. These acronyms stand for Energy Efficiency Ratio and Seasonal Energy Efficiency Ratio. Where COP is a unitless measure of useful energy divided by required energy input, EER and SEER achieve the same goal, but with units of BTU/Wh. Since heat is typically measured in BTUs and electrical work in kWh, these units provide more of a sense of what you are gaining in comparison to what you have to pay. To convert from COP to EER, the COP is multiplied by the conversion 3.413 BTU/Wh. COP and EER are both measured with respect to fixed evaporator and condenser temperatures; in an air source heat pump this would be the

seasonal minimum temperature and the indoor conditions. The SEER instead uses a variety of temperatures from throughout the year so as to provide a better sense of what the overall heat efficiency of the system will be. It is important to understand that these ratings are for the condenser, evaporator, and compressor alone. Inefficiencies related to poor system sizing, slipshod duct work, improper refrigerant charging, and restricted air flow are not accounted for in SEER ratings.[iv]

In addition to these ratings, efficiency for cooling systems is often measured in kW/ton. One ton of cooling is equal to 12,000 BTU/hr being removed[v].

The following picture shows a typical outside heat exchanger used in these systems. In the winter this unit acts as the evaporator, extracting heat from the outside air while in the summer this unit acts as the condenser, rejecting heat to the surrounding air. The fan located on the top pulls air through the unit increasing the overall heat-transfer properties of the unit.

Figure 2. Conventional Heat Pump Outside Air Unit

Four lines can be seen entering the outdoor unit: the electrical power line, the electrical signal line, the saturated vapor line, and the saturated liquid line. In heating mode, the high-pressure saturated-liquid refrigerant is pumped from inside the house out to the evaporator in the smaller diameter copper line seen above. The electrical signal turns the fan on and outside air is drawn across the evaporator. Heat is extracted from the air as the saturated liquid changes phase to saturated vapor. This vapor then travels through the larger diameter insulated line back into the house. The insulation helps to prevent heat loss from the saturated vapor in the cold outside line. The saturated vapor is then runs through the compressor before reaching the condensing coil in the air-handling unit. Here the heat is rejected as the refrigerant changes back to a saturated-liquid state and begins the cycle again.

In cooling mode, the process is essentially reversed; the heat exchanger outside functions as the condenser, while the coils in the air handler function as the evaporator. Depending on the local climate, systems may have the compressor inside or outside. The work from the compressor is ultimately rejected as heat; therefore it is desirable to have this outdoors if the cooling season is far more demanding than the heating season. By the same logic, it is desirable to have the compressor indoors in areas where heating loads are dominant.

4 Geothermal Heat Pumps

4.1 Ground Temperatures

A geothermal heat pump is designed to take advantage of more stable ground temperatures; lower condenser temperatures in the cooling cycle and higher evaporator temperatures in the heating cycle. Geothermal temperatures do not vary seasonally as drastically as air temperatures do. Ground temperatures are a function of depth, season, soil structure, soil moisture, and several other variables. The following chart shows seasonal ground temperatures as functions of depth and season in the state of Virginia (Geo4VA, 2006).

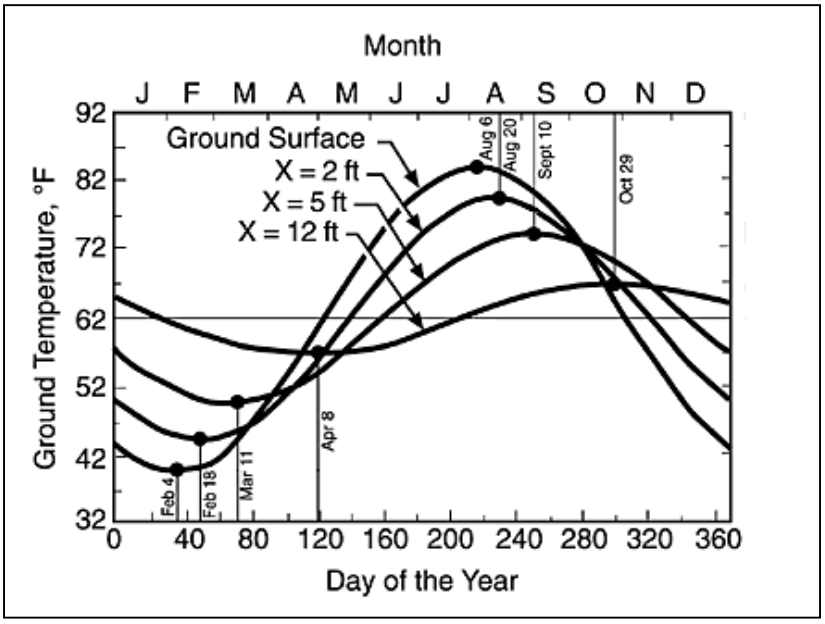

Figure 3 Ground Temperatures vs. Time and Depth

As can be seen in the figure, the winter soil temperature at a twelve foot depth fluctuates between 68 °F and 58 °F. In the summer it varies in the same range. Note that the maximum soil temperature at a twelve foot depth does not occur in the summer, but lags and occurs in

late October. Similarly, the minimum soil temperature at this depth occurs in early April. Groundwater temperatures achieve similar, and often more stable, temperatures as the soil temperatures shown above.

The link between efficiency and heat-exchanger temperatures is evident from the previous description on ideal heat pumps. The greater the difference between the evaporator and condenser temperatures, the greater the difference in saturation pressures in these heat exchangers. Higher pressures cause for increased compressor work. The relationship between required work and pressure is non-linear; each pound of pressure increase becomes more expensive than the last. Geothermal temperatures will cause for more efficient compressor operation than those available from a more conventional air-to-air system.

4.2 System Types

Geothermal systems are defined by the type of heat exchanger used for transferring heat with the ground and the nature of the heat carrying fluid. Systems will either use an "open" or "closed" heat exchanger. Open systems use water from the environment, extracting or rejecting heat to the water, and then discarding the water back into the environment. Closed systems cycle water through a constructed geothermal heat exchanger which transfers heat with the ground. Open systems take advantage of the more constant temperature of groundwater by using the groundwater itself as the transfer fluid. Closed systems are not limited to sites where groundwater is accessible and typically do not require the same level of permitting as they do not have the same likelihood for contaminating the environment.

4.2.1 Open Systems

Open systems require access to a water source, typically using groundwater. This water is abstracted from the ground, heat is exchanged with the heat pump, and then the water is disposed of. The choice for disposal method is dependent on the recharging rate of the aquifer as well as local regulations. Disposal to surface waters is an option only when aquifer recharging rates are far greater than the required flow rate for the system, so as to avoid depleting the reservoir. Local environmental regulations must permit the discharge of the water after the use in the heat pump as well. Reinjection into the aquifer is a far more common practice in open groundwater geothermal heat pumps (Banks, 2008). The location and depth of reinjection can have significant impact on the overall efficiency of the system. In cases where groundwater flow is well understood, it is recommended that the water be reinjected "downstream" in the aquifer so as to reduce the thermal interaction between the abstracted and reinjected water streams. The following figure shows an open reinjection geothermal loop (FHP, 2009).

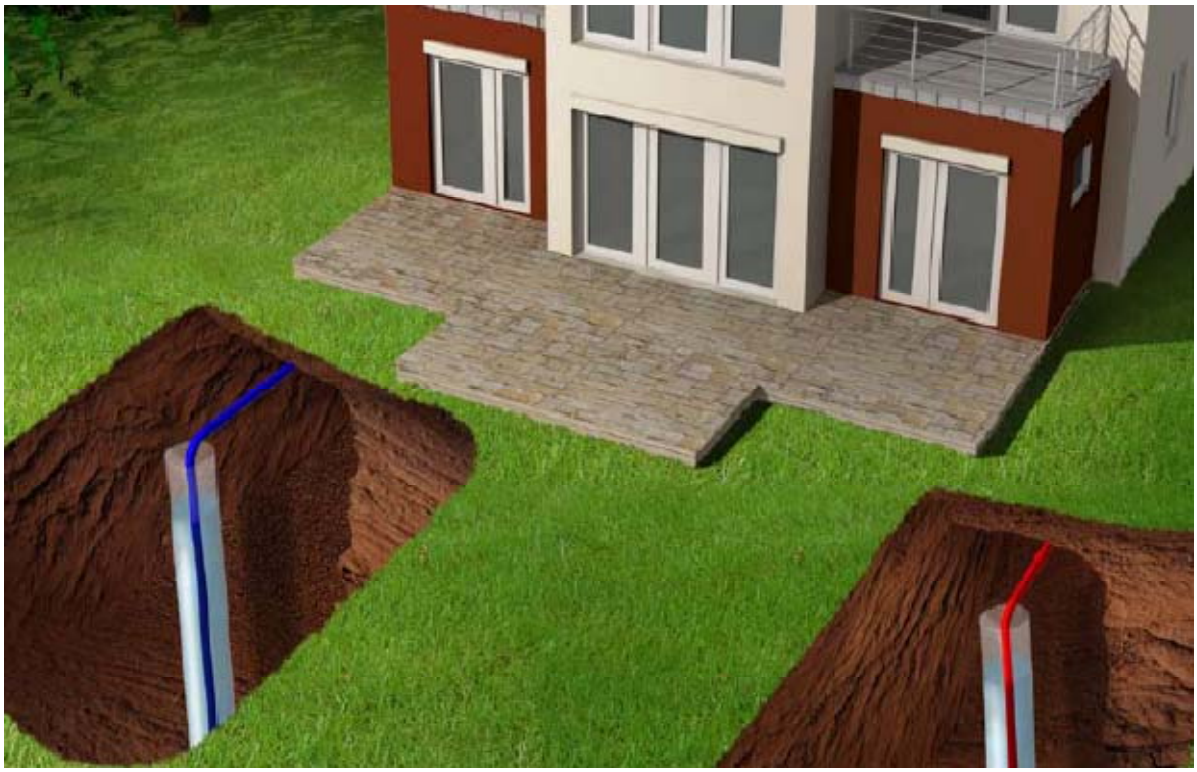

Figure 4 Open Reinjection Geothermal Loop

Open groundwater systems have several advantages over closed systems: they don't require the construction of a heat exchanger in the ground, they utilize naturally occurring convective groundwater flow rather than soil thermal conduction, and they can be coupled with a potable water system. However, open systems require that a useable source or water, both thermodynamically and logistically, be accessible. Open systems run the risk of interfering with the groundwater supply, requiring more in-depth and costly hydrologic engineering. These systems are also far more dependent on the geology of the region.

4.2.2 Closed Systems

Closed systems require the construction of a sealed and buried heat exchanger which can transfer heat with the surrounding soil and rock. These systems operate on conduction as the primary mode of heat transfer. They are divided into two types: direct circulation and indirect circulation. The heat exchanged with the ground will either be used to change the phase of the refrigerant directly, or it will be used to heat a fluid which will travel to the respective heat exchanger in the heat pump, indirectly changing the phase of the working refrigerant. Due to regulations with refrigerants, indirect closed systems are far more common than direct systems; indirect systems minimize the quantity of refrigerant required and the potential for leaks. Indirect systems also eliminate the potential for refrigerant flow problems. Lengthy heat exchangers, where compressor oil may enter the heat exchanger and build up, can create serious impediment to flow.

The following figure shows an indirect closed geothermal system (FHP, 2009).

Figure 5 Indirect Closed Loop Ground Source Heat Pump

The reliance of conductive heat transfer of these systems had them initially constructed out of copper by many installers. However, it was soon shown that the soil resistance to heat conduction dominates the overall heat transfer coefficient. This, along with concerns of mechanical failure, corrosion, and, most significantly, cost, has lead to the use of polyethylene plastic piping in closed system geothermal heat exchangers (Banks, 2008).

4.2.3 Heat Exchanger Types

Closed system geothermal heat exchangers can be classified as vertical, horizontal, and surface-water. Figure 5 shows a horizontal heat exchanger. Figure 6 shows a vertical geothermal heat exchanger, on the left, and a surface-water geothermal heat exchanger on the right (FHP, 2009).

Figure 6 Vertical and Surface-Water Heat Exchangers

Choosing the proper heat exchanger depends largely on the existing resources, available land, and available equipment. It is important to properly size the piping to allow for a large surface area and to maintain turbulent flow in the pipe. Soil heat exchangers should be at least 3 ft deep and not deeper than 15 ft. The maximum depth is important both economically and thermodynamically as deeper trenches are more expensive and they limit solar interactions for the heating season. Shallow geothermal heat exchangers can be thought of as essentially massive, low-temperature solar collectors (Banks, 2008).

Surface-water heat exchangers are recommended to be at a depth of no less than 9 ft. This is to ensure the variation in temperature is minimal and that the heat exchanger is somewhat insulated from the air temperatures above the surface (Banks, 2008).

Attention should be given to the effects of changing surface water temperatures. Although it is unlikely in smaller residential systems, thermal pollution can caused dissolved oxygen levels to drop (in the heat pump cooling cycle) or rise (in the heating cycle), altering the ecosystems drastically. Thermal pollution has been the basis for litigation in this country and it is critical that its impacts are understood before surface waters are used as either sinks or sources for thermal systems.

5 Data Collection

A residential HVAC system brings in air, conditions it, and pushes the air back into the conditioned space. Treating the HVAC unit as a control volume, the inputs are air, electrical energy, and a convective fluid to act as either a heat source or sink. The outputs of the system are conditioned air and the convective fluid[vi]. In the case of the air-to-air system, this fluid is outside air. In the case of the geothermal system, this fluid is groundwater or water from the geothermal heat exchanger.

In order to determine the values needed to calculate the COP of each system, we need to determine the values for Q_{out}, Q_{in}, and W_{in}. To accomplish this, the HVAC unit was treated as a control volume. The various inputs and outputs described above were monitored and recorded. The following pictures show the control volume and the respective inputs and outputs of System B during the cooling season. The groundwater is being heated by the unit as the air in the air handler is being cooled and dried.

The electrical work input is consumed in the compressor and the electric strip heating elements. The strip heat has a significant effect on the efficiency and is

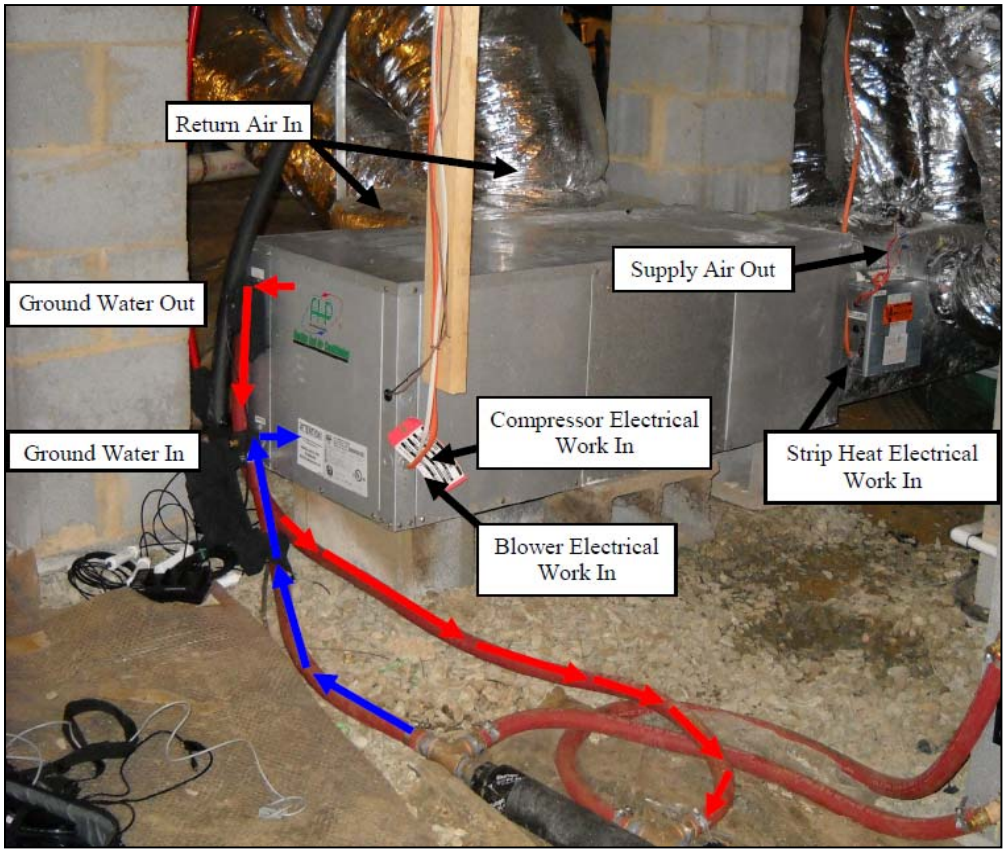

Figure 7. System B: Residential HVAC Unit as a Control Volume During Cooling Cycle

5.1 Electrical Work

Electrical work was monitored using current transducers and data loggers. The current transducers were placed around one of the electrical supply lines. By sensing changes in magnetic flux from the alternating current of electricity on the wire, the current transducer sends a signal to the data logger signifying how much current is flowing. Using Ohm's Law, the current, I, and supply voltage, V are multiplied to give the power, P, consumed by the monitored unit.

$$P = I \cdot V$$

Supply voltages were measured on site and assumed to be constant through the duration of the testing. Figure 8 shows the current transducers and data loggers used to measure the compressor and blower power for System B.

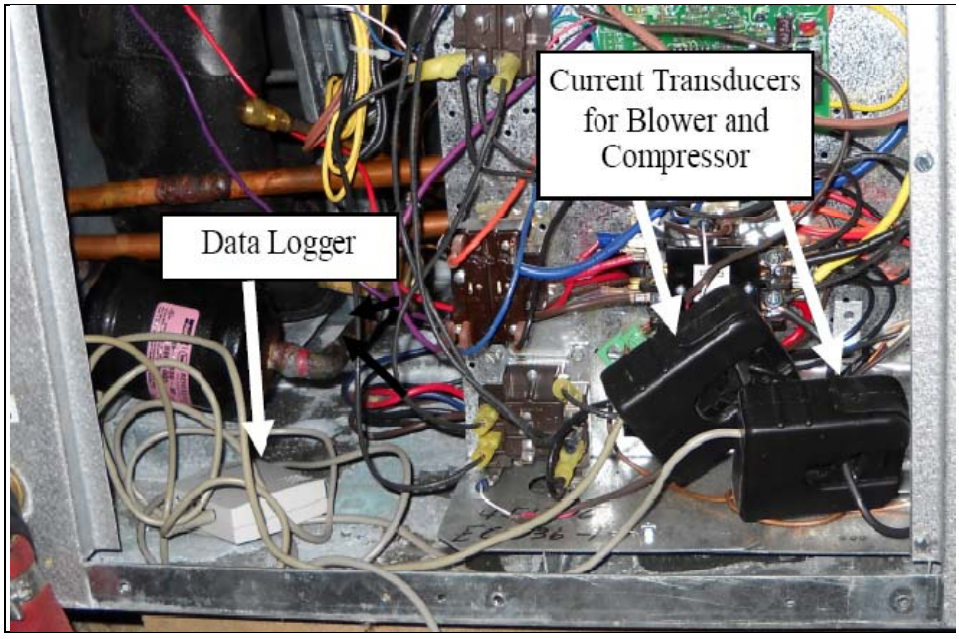

Figure 8. Current Transducer and Data Logger

Due to a limited number of transducers of appropriate size, the geothermal loop pump and HVAC control systems were not logged. The choice to log the compressor, blower, and electric strip heat rather than the pump and controls was based on several factors:

1. The head loss in the geothermal loop should remain essentially fixed as the water temperature is the only variable in this loop and it does not vary more than 15-20 °F. This has a negligible effect on the density of the water. This suggests that the load on the geothermal pump should be fairly fixed.
2. The head loss in the duct system will change as registers are adjusted, doors between registers and air returns are opened or closed. The density of the air will vary far more significantly than that of the geothermal loop water.
3. The compressor is the most significant load in the system and will vary greatly.
4. The electric strip heat represents not only a large load, depending largely on weather conditions, but one that is very expensive. If electric strip heating loggers showed frequent use of the heaters, the economics and overall environmental impacts of the geothermal system would be unfavorable, most likely due to improper system sizing.
5. HVAC controls do not represent a significant load. This load is believed to be several orders of magnitude smaller than that of the compressor.

5.2 Air Flow

Air velocities were measured using an Alnor hot-wire air-velocity meter. This unit monitors the electrical power required to keep a small piece of wire heated to a predetermined temperature. The unit uses this electrical load to determine the convective heat loss from the wire. This correlates directly to an air velocity. The precision of the device was tested by taking several different readings over the course of the study. During similar operating conditions, the hot-wire anemometer proved consistent. The accuracy was tested by comparing readings with those from a vane anemometer. Readings from these two devices varied no more than 4%. The hot-wire anemometer had been professionally calibrated within the past 10 months. Figure 9 shows these two devices measuring air flow in one of the return ducts on system A.

Figure 9 Hot-Wire and Vane Anemometers

Measurements were taken at different points on the filter surface so as to provide a matrix of readings which could then be averaged. These velocity matrices, along with return duct measurements, are shown in Appendix A.

The volumetric air flow was calculated as the product of air velocity and the cross sectional area of ductwork at the velocity measurement. Mass flow rates, $\dot{m}$, were then calculated by multiplying the volume flow rate by the density, ρ. Densities were calculated using psychrometrics as described in Appendix B.

5.3 Air Enthalpy

Air enthalpy was calculated from dry bulb temperature and relative humidity. Dry bulb temperature and relative humidity were monitored on regular intervals from inside the air handler supply and each of the returns. Figure 10 shows the data logger used to measure air handler supply conditions. Return air conditions were collected by a similar logger placed in the return ductwork.

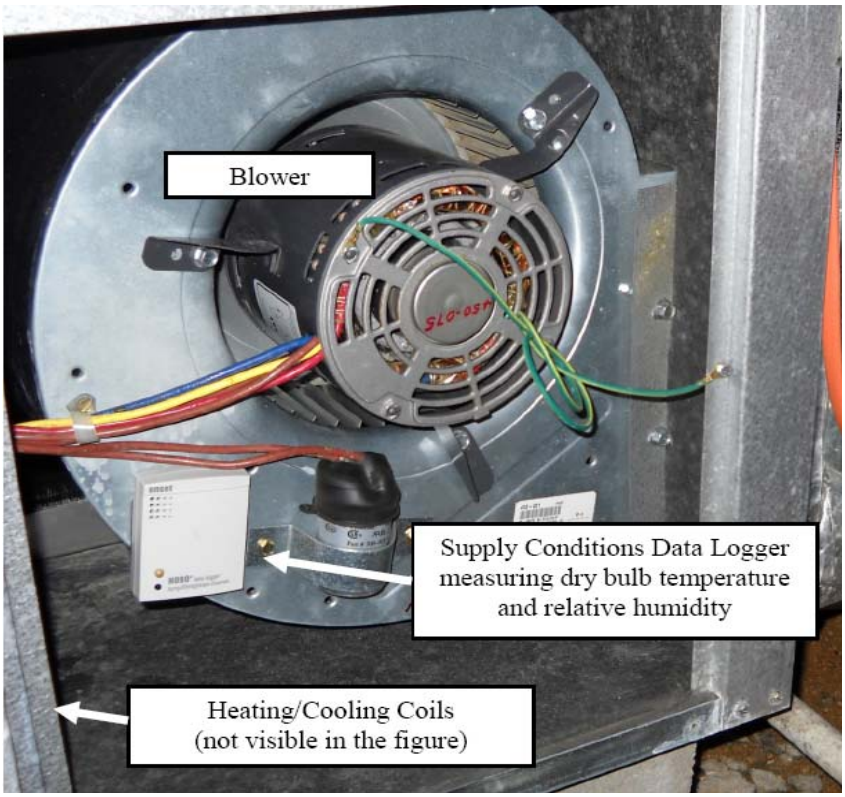

Figure 10. Air Handler

Using the dry bulb temperature and relative humidity, the various parameters needed for the study were calculated using psychrometric relations. These calculations are detailed in Appendix B.

5.4 Groundwater Temperatures

The temperatures of the groundwater were logged using stainless steel temperature probes. These devices act as a thermistor; a temperature varying resistor. The variance in resistance correlates directly with a temperature which can be logged by the data logger. Penetrations were not reasonable in these systems. Therefore, it was not possible to immerse the probes in the fluid nor create a thermowell fitting in the pipe. Instead, these probes were fixed to the outside of the brass geothermal fittings on the air handling unit and wrapped in layers of cloth to act as insulation. The figure below shows the probe inserted into a cloth wrap around the geothermal inlet into the unit. The photo was taken prior to insulation in order to have the probe remain somewhat visible.

Figure 11 Geothermal Water Temperature

5.5 Water Pre-heat Temperatures

The geothermal heat pumps studied had a water pre-heater ("desuperheater") installed to further increase the efficiency of the system. These units take advantage of high temperature superheated vapor leaving the compressor. This vapor is cooled to saturation temperature using domestic hot water. The heat recovered is a function of the flow rate and temperature rise of the domestic hot water. Flow rates were not obtained from the system itself. Manufacturer's data from the pump was obtained and used to estimate the flow rates. The domestic hot water temperatures from before and after the desuperheater were measured using stainless steel temperature probes similar to the ones used to measure the groundwater temperatures.

Unfortunately, the temperature probes needed for this were not available for System A during the cooling season. Due to limitations in the system size, the water preheater is not used in System A during the winter months. The data from System B is all that was collected and analyzed.

5.6 Overall Data

Data sets were collected from each system. Due to scheduling conflicts and a few errors in the logger interval programming, the data sets vary in time, number of data points, and intervals between points. Table 1 shows these values for each of the data sets.

Table 1 Data Sets Information

Date Set	Start Time	End Time	Interval (seconds)	Duration (days)	Data Points
System A Cooling	7/24/09 2:00 PM	8/8/09 3:18 PM	90	5.2	4,954
System A Heating Short	2/5/10 10:00 AM	2/5/10 11:11 AM	1	0.0	4,019
System A Heating Long	9/23/09 12:00 PM	1/6/10 12:27 AM	420	105.5	21,703
System B Cooling	9/7/09 12:00 PM	9/12/09 3:51 PM	120	15.1	10,839
System B Heating Short	2/5/10 2:30 PM	2/5/10 3:36 PM	1	0.0	4,285
System B Heating Long	10/16/09 2:00 PM	1/30/10 2:01 AM	420	104.5	21,501
System C Cooling	9/20/09 2:00 PM	10/5/09 3:47 PM	60	15.1	21,707
System C Heating	2/15/10 9:00 PM	3/2/10 7:00 AM	60	14.4	20,760

5.7 Manufacturer's Data

The collected data was compared to the heat pump manufacturer's data. The manufacturer's information was rated in BTU/hr and EER for the cooling. These were converted to tons and COP respectively. The table below shows the size and COP for each system according to the manufacturer (FHP, 2009).

Table 2 Manufacturer's Data on Geothermal Units

System	Cooling Capacity	Heating Capacity	Cooling COP	Heating COP
A	4 tons	58,000 BTU/hr	5.6	4.2
B	3.2 tons	31,500 BTU/hr	7.0	4.4

This performance data is measured according to ARI/ISO standard 13256-1. The inlet temperature for the geothermal test water is held constant at 59 °F in the summer and 50 °F in the winter.

6 Data

6.1 Cooling Season

The first data collected was from System A during late July and early August. A subset of the data is shown in Figure 12. This data shows the expected drop in supply air temperature when the compressor is in operation. The temperature drop is accompanied by a rise in relative humidity. Relative humidity is defined as the ratio of vapor pressure in the air and the vapor pressure in saturated air at that temperature. Since saturation vapor pressure decreases with air temperature, the overall relative humidity should increase up to a maximum of 100%. This is when condensation occurs. In the figure, 100% is not reached. However, this is believed to result from coil bypass and because of the position of the data logger. Coil bypass represents the quantity of air which is not contact the coil surface and thereby may not reach saturation. Figure 10 shows the logger attached to the side of the blower. It is believed that the air temperature of air which does contact the coil may change slightly between the cooling coils and the blower, thereby changing the saturation pressure and relative humidity.

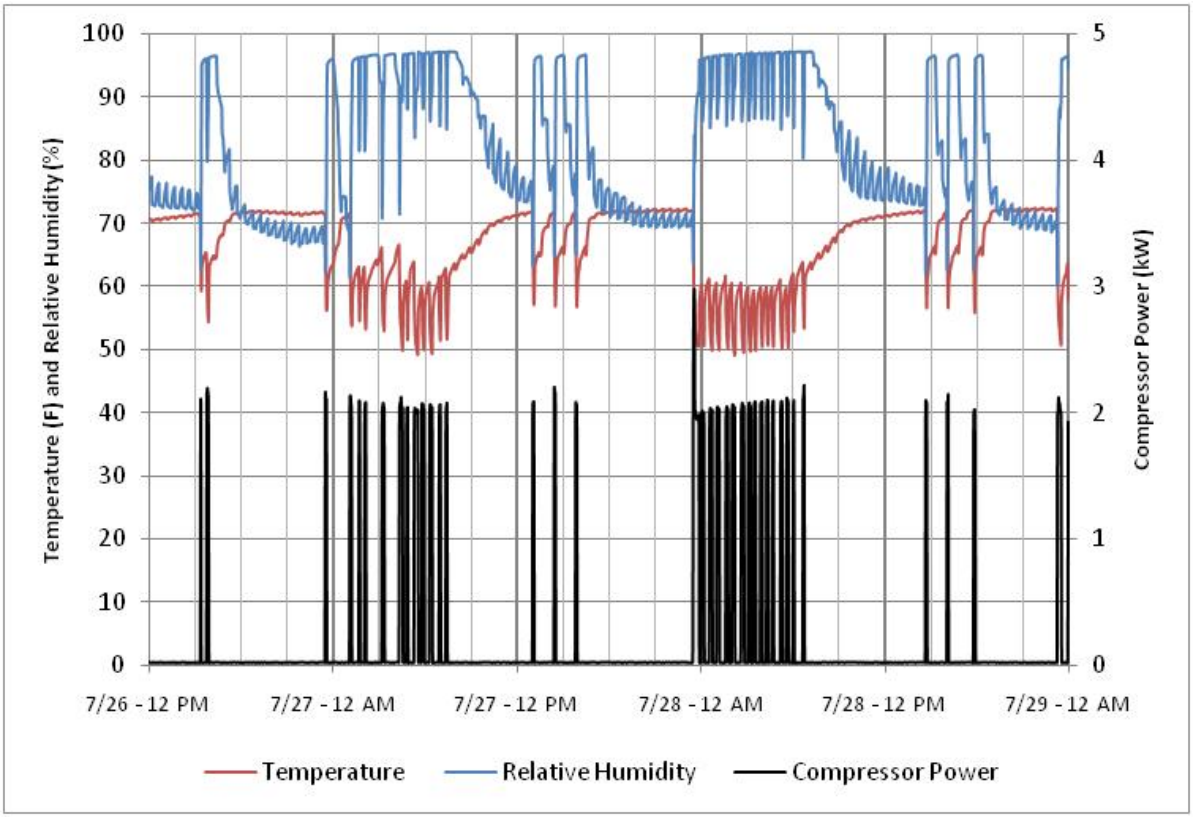

Figure 12 System A: Air Supply Conditions and Compressor Power

The temperature and relative humidity changes are expected, but they do not relay anything about the change in enthalpy across the cooling coils. Both geothermal systems have two return ducts and one supply duct. With each duct having its own temperature and relative humidity, there are six inputs needed to determine the enthalpy change through the air handler (3 temperatures and 3 relative humidities). In order to simplify this visually, enthalpies are calculated (again using methods from Appendix B) and shown, along with compressor power, in Figure 13 below.

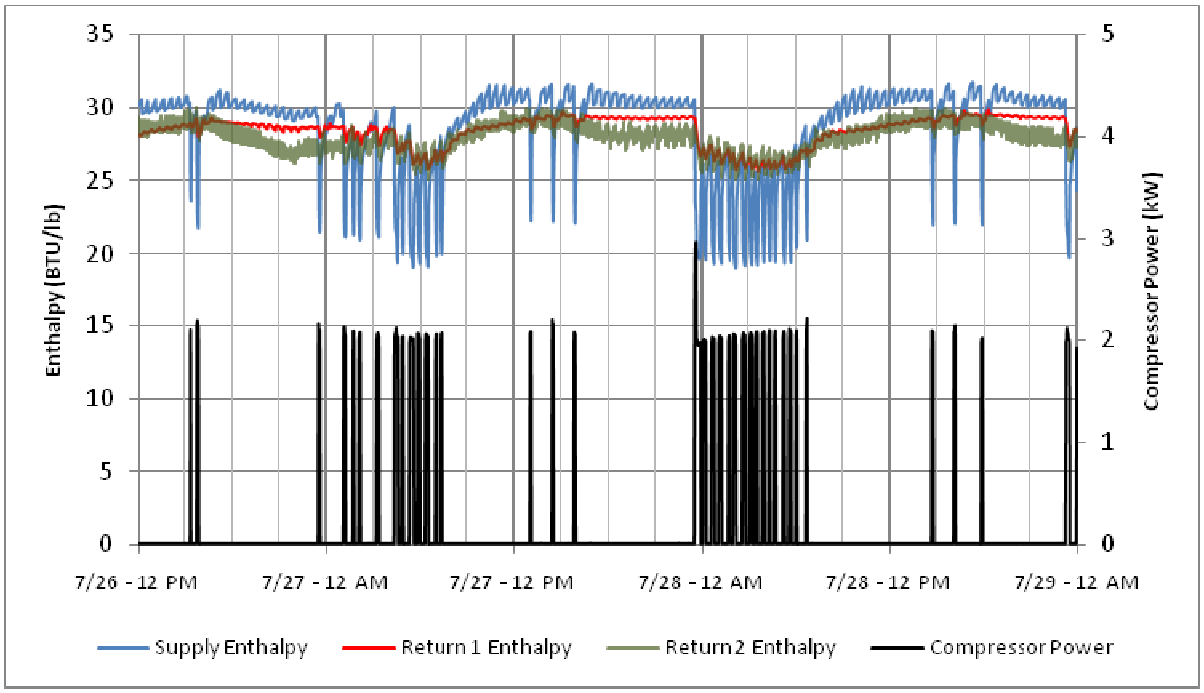

Figure 13 System A: Air Enthalpies and Compressor Power – Cooling Season

From this data, the compressor is operating in the 2.0 – 2.2 kW range. This is a 4 ton unit. This would seem to suggest that the system was operating with an efficiency of 0.55 kW/ton. However, it can be seen in Figure 14 that the unit is not providing 4 tons (48,000 BTU/hr) of cooling at any time over this period.

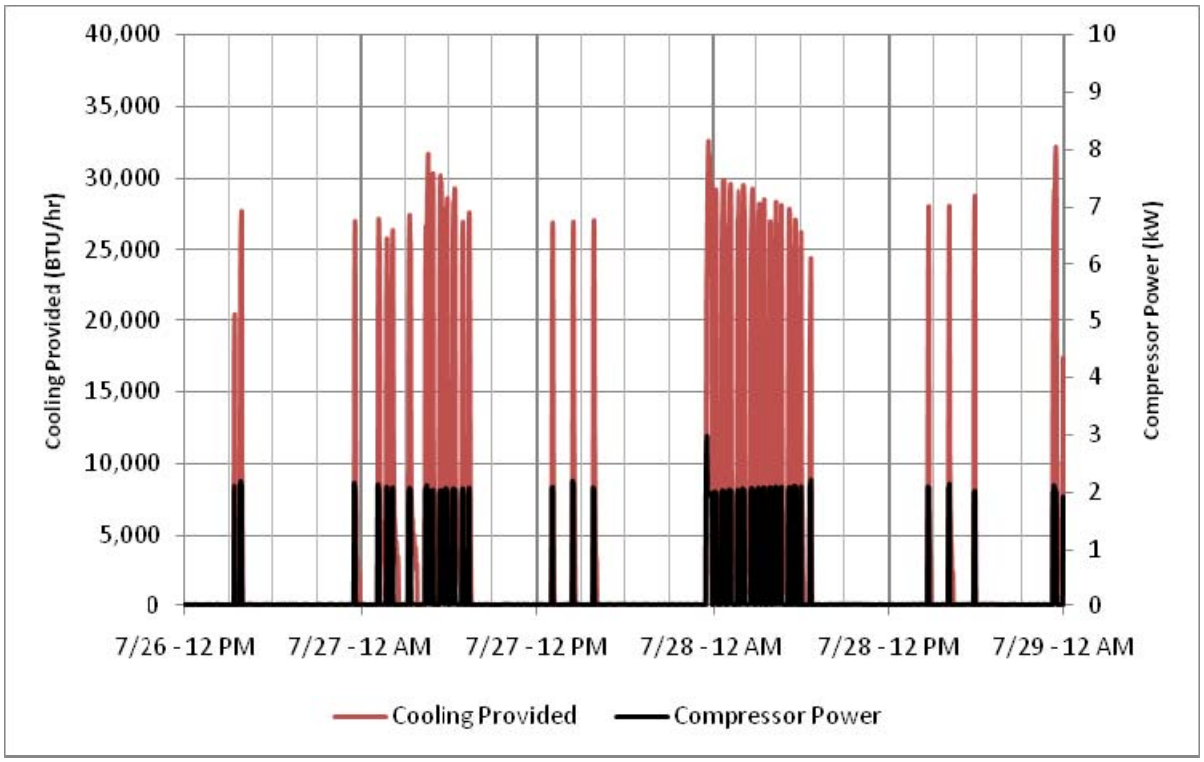

Figure 14 System A: Cooling Provided and Compressor Power Used

Instead, this unit appears to be operating at around 1.0 kW/ton. This efficiency is comparable to that of an average air-cooled unit.

The corresponding graph for System B, shown on the following page, suggests an even lower efficiency for System B.

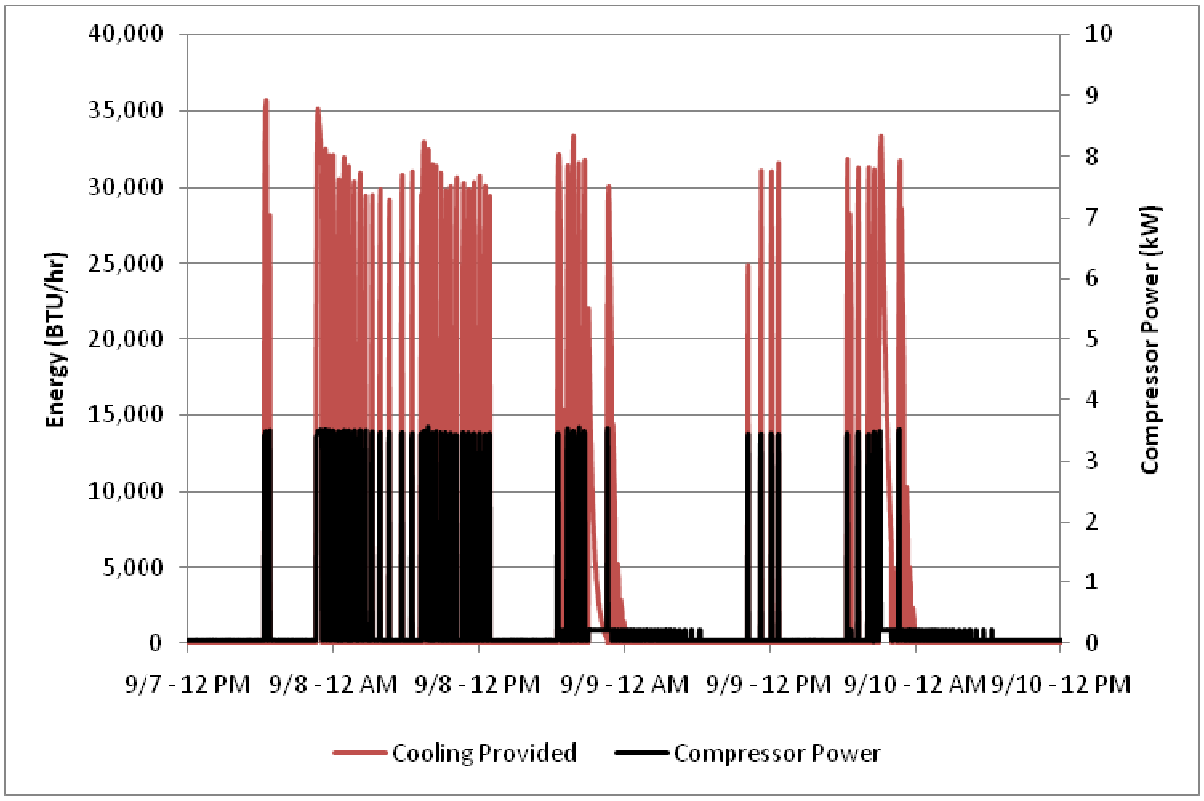

Figure 15 System B: Cooling Provided and Compressor Power Used

This system seems to be operating at nearly 1.6 kW/ton. This is quite a bit higher than the average air-cooled unit, causing for suspicion in this data. Given that the efficiency is mostly driven by condenser temperatures in the summer, the geothermal water used to cool the units is one of the most significant variables in this data set. Groundwater temperatures from both Systems A and B are shown in Figure 16 and Figure 17 on the following page.

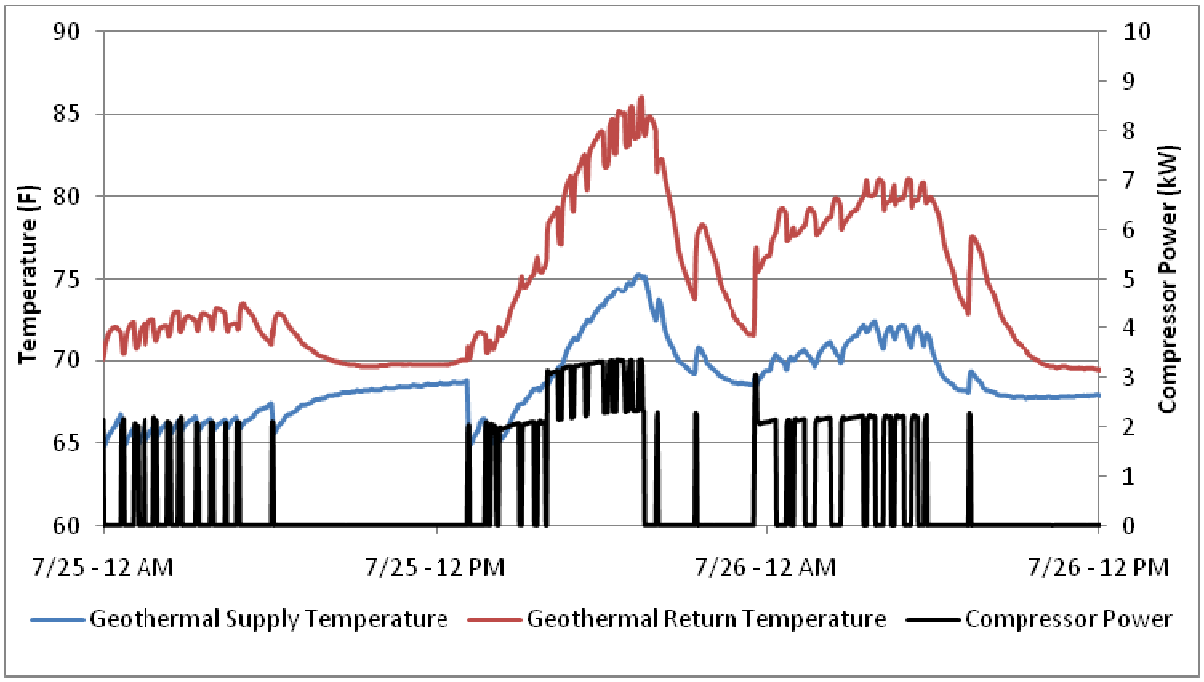

Figure 16 System A: Groundwater Temperatures and Compressor Power

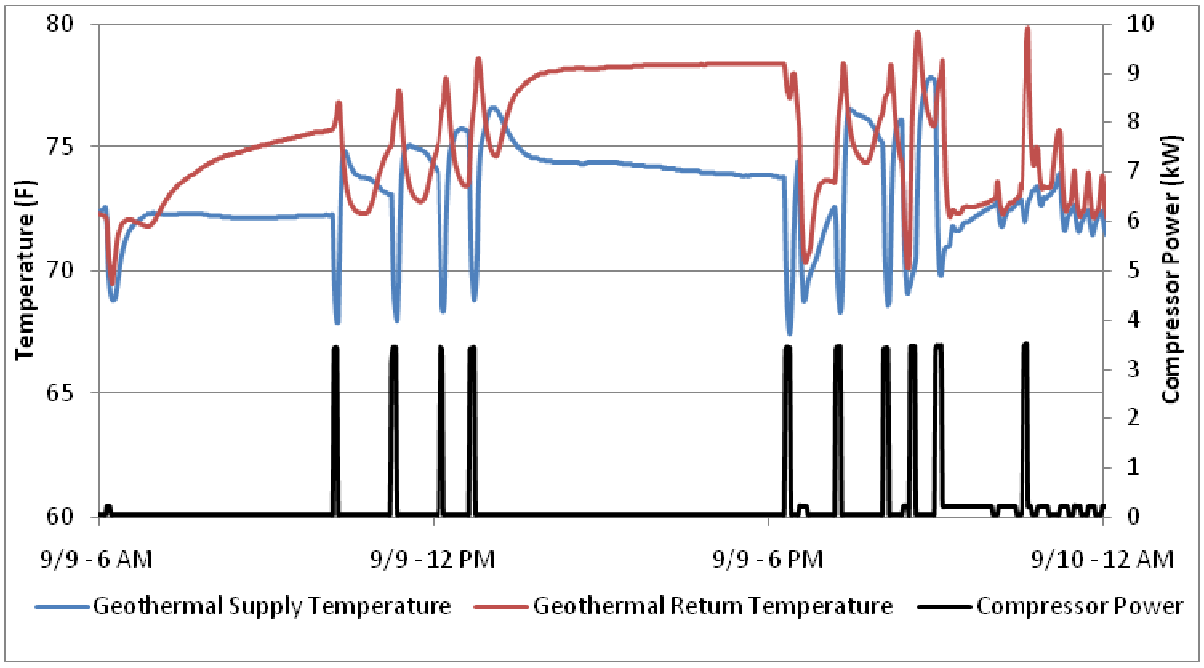

Figure 17 System B: Groundwater Temperatures and Compressor Power

The groundwater temperatures do not meet the design specifications for either system. It is important to note the dates for the cooling data here. System A temperatures reach far higher than those of System B, but it is from data collected in late July being compared to data from early September.

The average geothermal supply water temperature from System A was 68.0 °F while the system was running. The average from System B is 74.1 °F. These temperatures represent the temperature of the thermister, not the geothermal supply water. Although these are going to be close, the temperatures from System B will be skewed towards higher temperatures. The air handler unit in System A is located in conditioned, basement space, while the unit for System B is in unconditioned space which is surely hotter than 74.1 °F.

The efficiency data from the cooling season data is suspect given that the average geothermal supply temperatures are less than average outdoor temperatures. Outdoor air temperatures are the condenser's convective fluid temperatures in an air-to-air cooling system. It is not expected that the geothermal system performs as efficient as, or less than, the traditional air-cooled systems. It is believed that because of the nature of the system and the data logging intervals, the data represents general trends only. It is not sufficient for accurately quantifying efficiencies. This is believed to be a result of the transient nature of the system. This is discussed in greater detail further in the paper.

The remaining data is shown to display general trends in the systems.

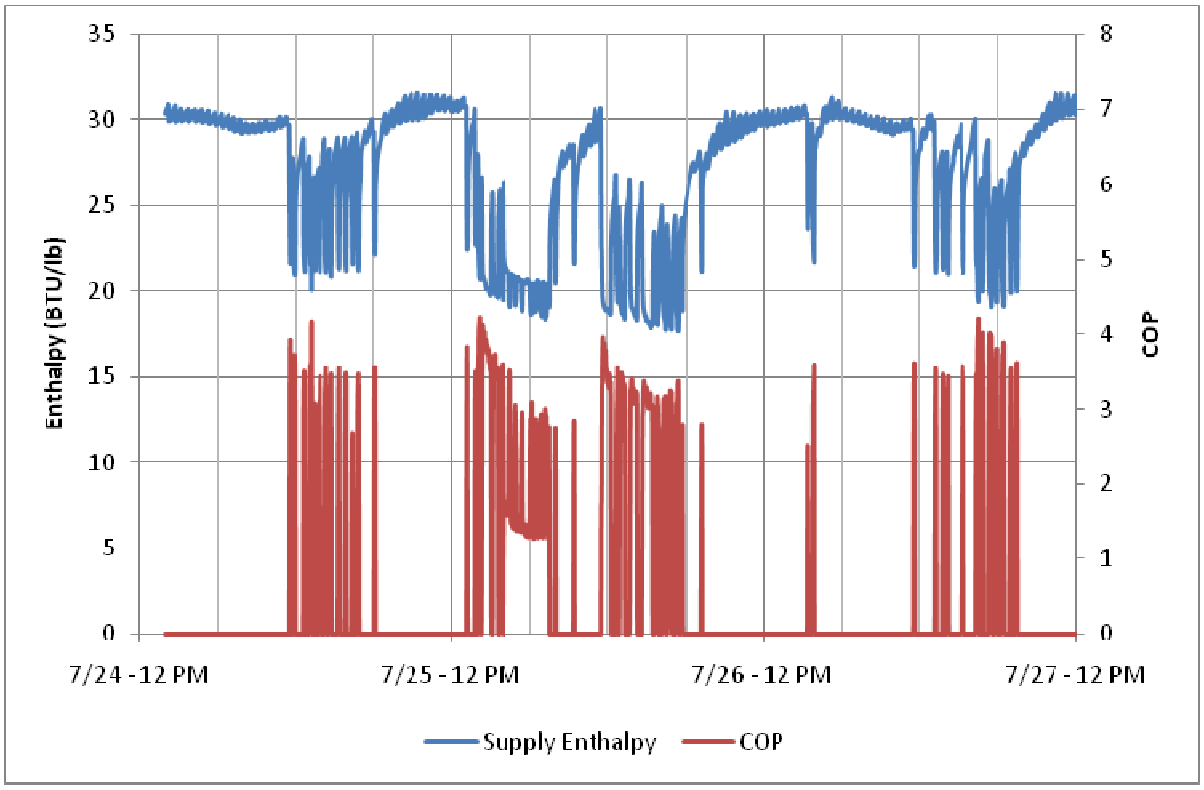

Figure 18 System A: Supply Enthalpy and COP - Cooling Season

Figure 18 shows the air supply enthalpy along with the calculated COP for System A. The COP value is not easily calculated and is based on a number of assumptions detailed in the short-interval heating data section of this paper. A "filter factor" was introduced in order to handle changes in the air flow rate over time. The choice of a filter factor is one of the most significant of these assumptions. This factor is assumed to be 75% for the graphs in this section. This means that the air flow rate averages 75% of the maximum measured flow rate.

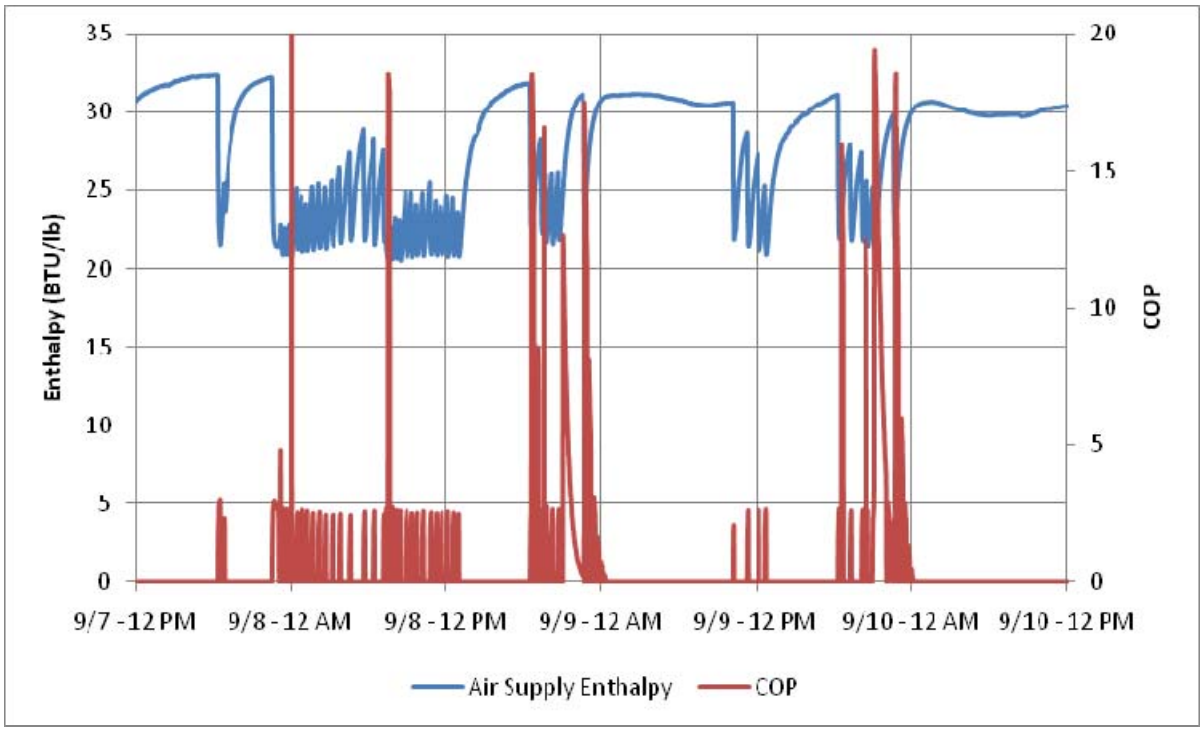

Figure 19 System B: Supply Enthalpy and COP – Cooling Season

System B has an overall average COP of 3.97 from the data above. However, the values above 10 and below 1 are believed to be outliers resulting from the system not reaching steady state. The transient nature of the system, along with the data logging time intervals, causes these outliers. When the data logger samples a point right after the compressor turns off, the coils are still providing a great deal of cooling when only the blower work is needed. Similarly, when the compressor is charging the system, a great deal of work is being supplied long before the evaporator reaches the desired temperature and provides significant cooling.

When these outliers are removed, by eliminating COP values less than 1 and greater than 10, the COP is reduced to 2.75, a reduction of nearly 31%! This is a significant change and needs to be addressed. An additional data set was collected at one-second intervals in hopes

of resolving this issue. This set was collected in order to capture all the work and all the benefits in this transient system at a much higher resolution. This data set is shown in a later section.

The overall average COP for System A during the cooling season was 2.56. When outliers were removed, as described above, the COP rose to 2.62.

Neither the calculated COP nor the manufacturer's COP values include the use of water-pre-heating desuperheater. This feature is optional on these units. From the calculations made from System B, the desuperheater saved 66,325 BTUs over a period of five days. This does not include the cost of pumping the water from the water tank to the desuperheater unit. This energy, over the time period measured, increased the overall COP of System B from 2.75 to 2.89; an increase of 5%. This increase in efficiency directly displaces electrical resistance heating that would otherwise have occurred in the water heater.

Several of the figures in this section have shown small cyclic variations in supply air conditions when the compressor is not operating. The variations in the temperature are believed to be caused by a faulty thermocouple in this particular logger. This would result in the fluctuations in relative humidity seen here. This is the only data set in which this activity appears. Similar data sets for Systems B are shown in the Appendices.

Cooling data from the air-cooled system, System C, was not collected. The attempt that was made occurred too late in the year to collect cooling data. As a result, it initially appeared to be reasonable heating season data, albeit at a higher efficiency than true winter operations

because of the relatively high outdoor air temperatures. However, the data which was collected is believed to be corrupt. This is explained in further detail along with the data in Appendix E.

6.2 Extended Fall/Winter Data

The data collected over the fall and winter was sampled every 7 minutes, and is shown in Table 1. This data set was collected in order to determine long term behavior of the system, in particular how often the back-up electric strip heat was needed. On the following pages, graphs show data representing the trends of these systems as fall turns to winter.

Although the data shows the overall trend in energy use, it is believed to be non-representative of the performance in terms of efficiency, again because of the outliers created by the longer time intervals.

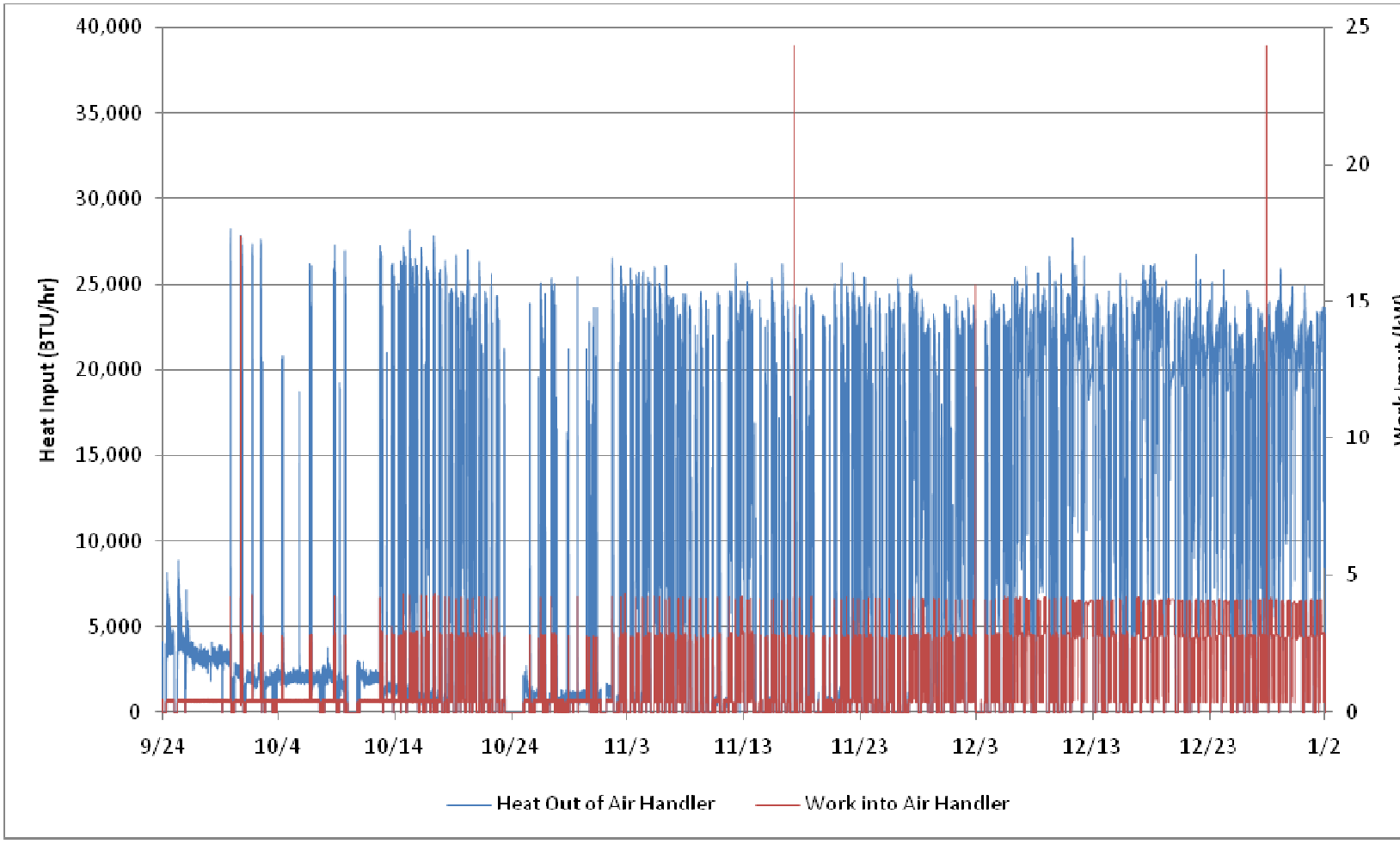

Figure 20 System A: Long-term Heat Output and Work Input - Heating Season

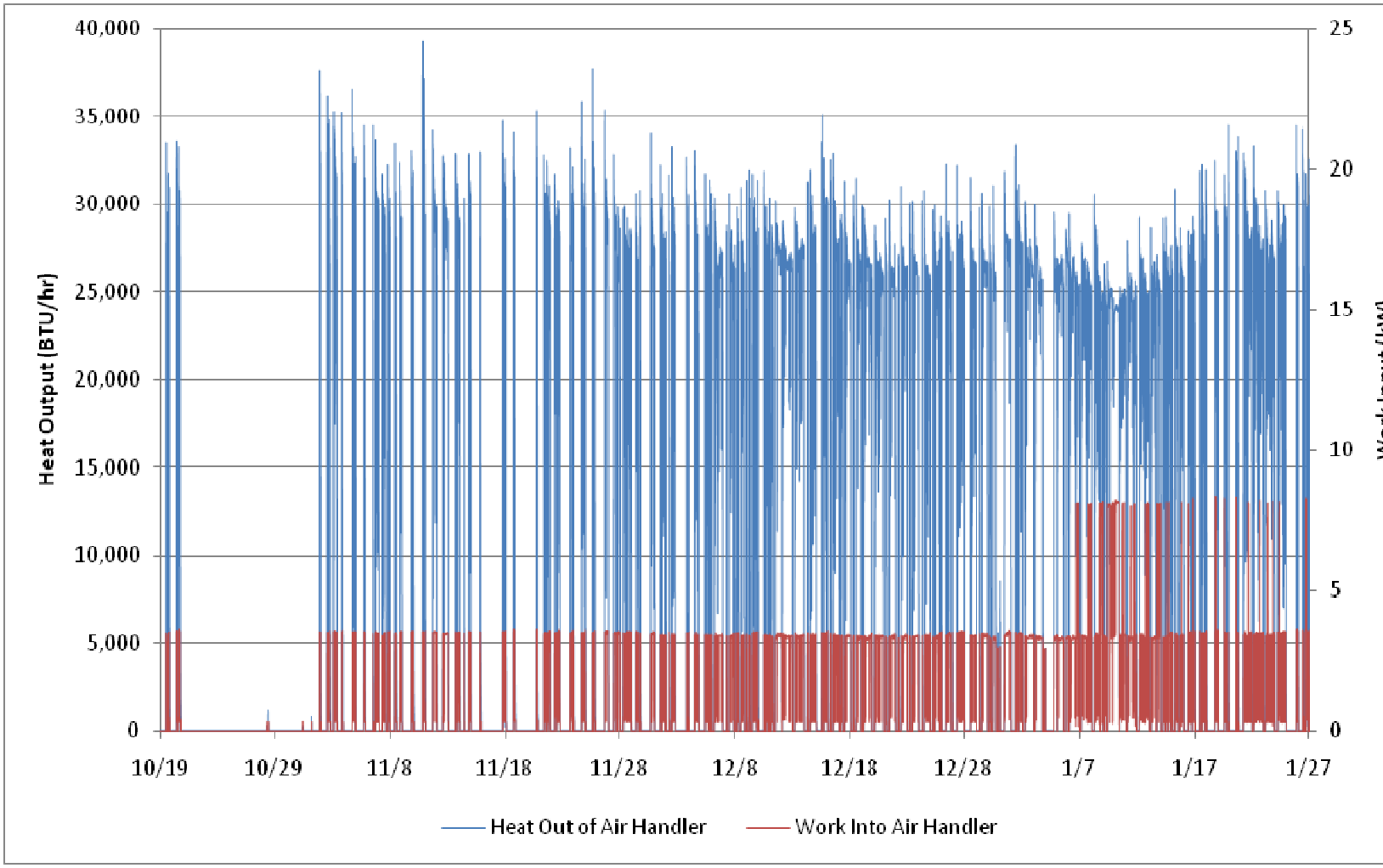

Figure 21 System B: Long-term Heat Output and Work Input - Heating Season

These figures present a visual aid in understanding the differences in the COPs of each system. While this data is not necessarily reliable when trying to quantify the differences in the COPs between the two geothermal systems, it does display a trend which supports the more quantitative data of the following section. The COP is represented by (but not equal to) the ratio of the blue line height to the red line height[vii]. The ratio of blue to red is higher in System B; the system which has quantitatively shown a higher COP.

System B shows an average COP over this period of 5.26, whereas System A shows a COP of only 2.96. This is largely the reason for believing that the short "snapshots" of the transient systems can be a large source of outliers. When the outliers were removed, as described in the cooling data section, the overall average COP of System B dropped to 2.75, while System A dropped to only 2.95. It is believed that one possible reason for a higher number of outliers in System B is that the heat pump cycle length appears shorter. This can be the result of many factors, most likely thermostat placement, thermal mass in the house, register location, and infiltration rates. A shorter cycle length increases the number of starting and stopping periods for the compressor. These periods are transient and produce the outliers in question. The cycle times can be seen in Figure 26 on page 60.

In addition to the differences between the magnitudes of the outliers, System B used a significantly larger amount of electrical energy starting in early January, as can be seen in the figure above. Data was not collected from System A in January. The more extreme weather conditions have the potential to increase the heating load beyond that which the heat pump can provide. This point is referred to as the balance point. It appears as though the balance

point for System B is reached in early January and therefore the backup electrical strip heat came on. This also likely happened in System A, but was not logged[viii].

Figure 22 below shows the average outdoor air temperature for each of the geothermal systems. The drop into the 30's in early January brought on higher heat loads for both systems. When the electric strip heat operates, the COP is affected negatively. The strip heat provides only electrical resistance as a heating method, reducing the COP for that particular heat to 1, thereby lowering the overall average. Despite this negative impact, the overall average COP for System B remained higher.

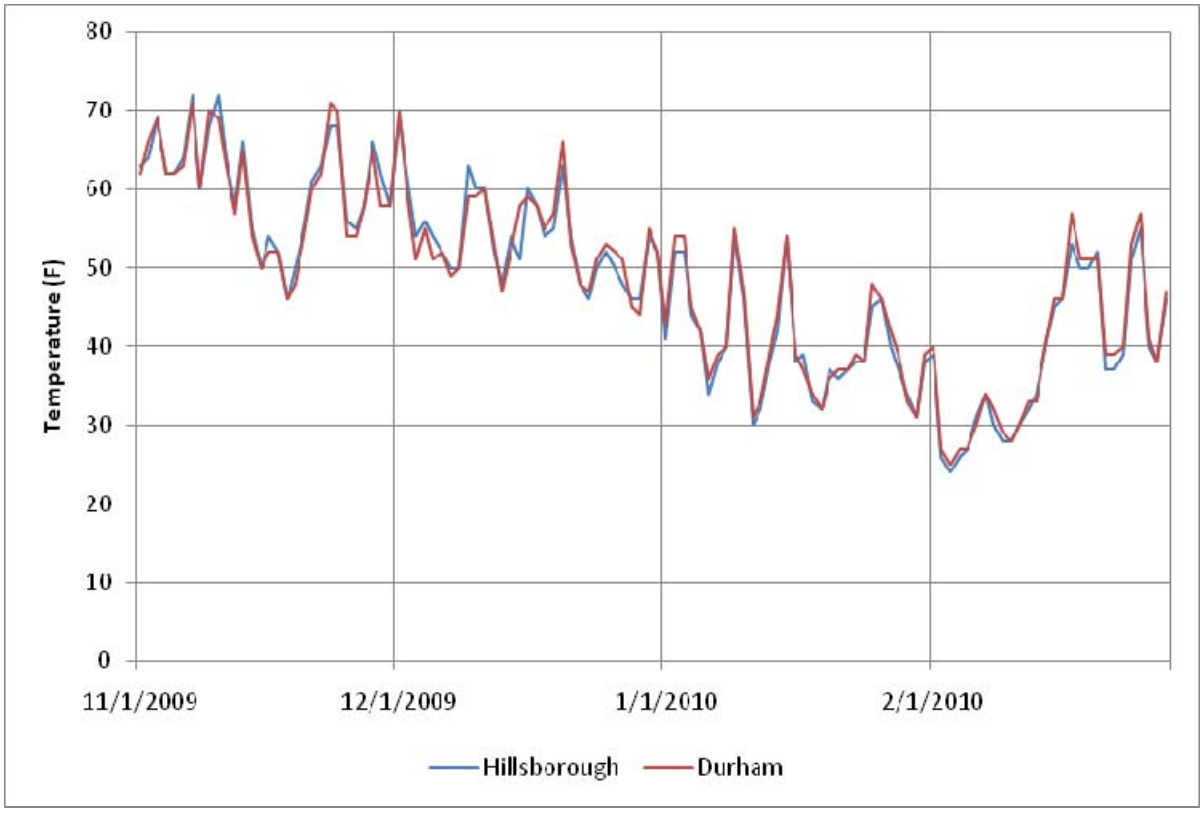

Figure 22 Average Outdoor Air Temperatures for System A (Durham) and System B (Hillsborough)

In order to determine COP values more accurately, data was gathered at one-second intervals for a one-hour period. The COP for these systems should not vary greatly throughout the year, with the exception of the need to use strip heat, because of their relative independence from air temperatures in the evaporator (or condenser during the cooling season).

Heating data from System C was analyzed in the same manner as the data from both System A and B. The data logging equipment for this system is believed to be faulty. The COP for the system was calculated to be 5.41 using a filter factor of 75%. The data from System C is not used, but is shown in Appendix E.

6.3 Short Interval Heating Data

This data was collected over a period of 1 hour at one-second intervals. This was collected to better understand how the system was operating with a higher level of resolution. As can be seen in Figure 23, the COP in System B becomes quite high once the compressor cuts off and the blower remains on. Clearly the system is not reaching a steady-state operation and the blower is able to remove heat from the air handler which has already been "paid" for in terms of work input. This is the exact transient behavior for which this data set was collected. This presents an interesting and pivotal problem for the study: when is it reasonable to assume that the system is delivering energy to the house?

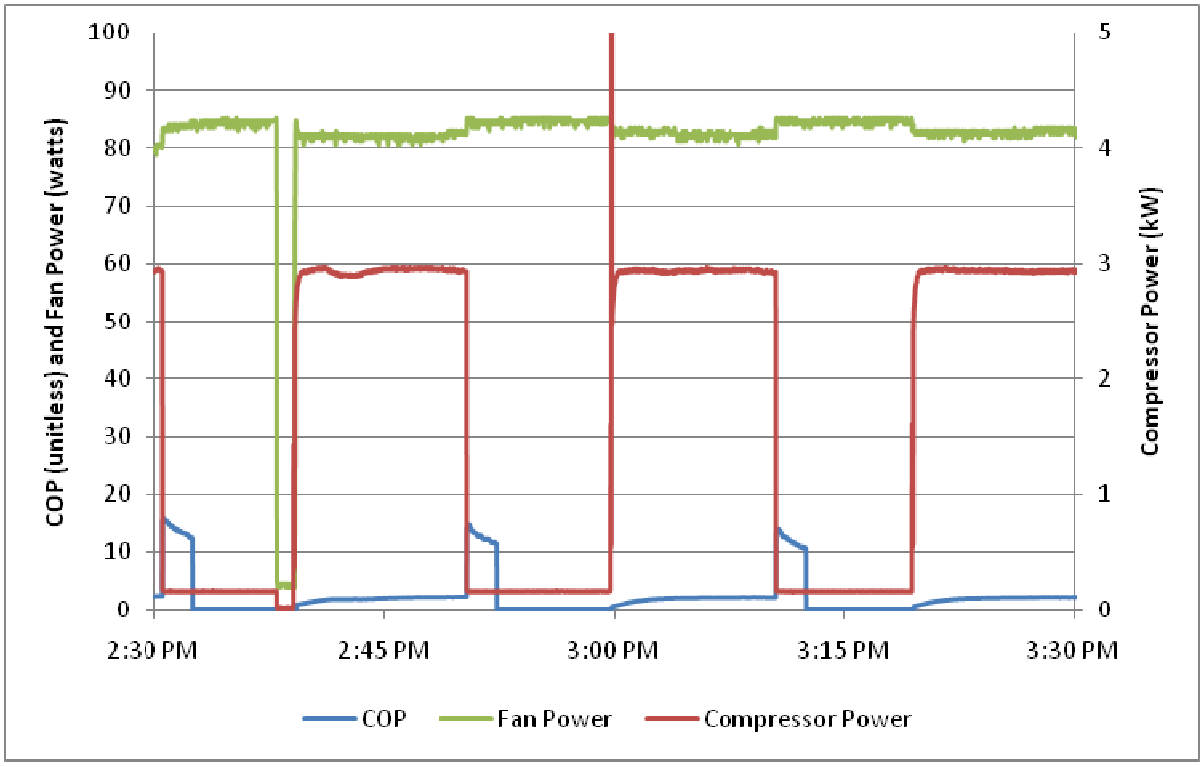

Figure 23 System B: Short Cycle COP, Fan Power, and Compressor Power

Initially, whenever the compressor was running the system was considered to be on and delivering energy. During one of the visits to System A, the fan run time was compared to the compressor run time. The fan stayed on for just over two minutes after the compressor turned off, continuing to extract heat from the coils. In the figure above, it is apparent that the fan stayed on in System B for nearly all of the time monitored. The calculations for COP were therefore initially based on when the fan was running.

However, this was changed when one data set showed suspect fan power data. It was then decided that the system would be considered in operation while the compressor was running and two minutes following compressor shutdown. For the systems without corrupt blower data, the overall average COP did not change significantly, suggesting reliability and consistency in using this method.

Figure 24 below shows the amount of energy delivered from the air handler in comparison to the electrical work input into the compressor. Here again it can be seen that the energy delivery process has a ramp-up and ramp-down period.

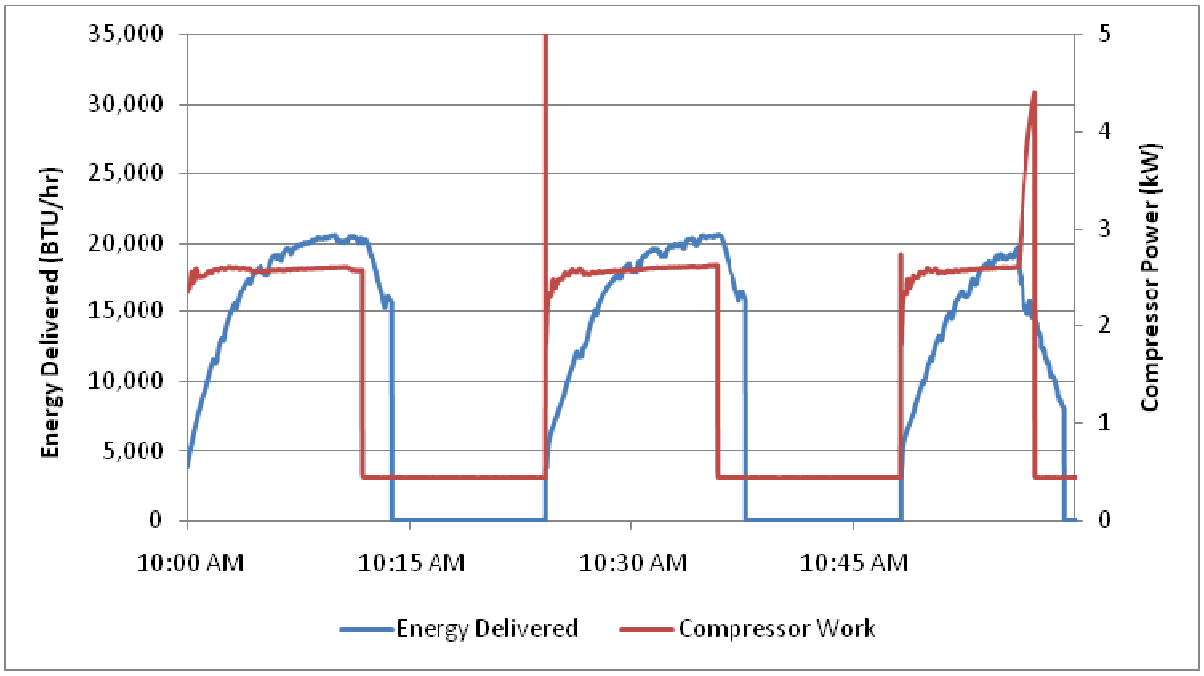

Figure 24 System A: Compressor Power and Energy Delivered in the Air Handler

All calculations were carried out using Microsoft Excel. The data were compared on a moment-by-moment basis. The following table displays a 30-second period in the operation of System B.

Table 3 System B Energy Flow and COP Data

Time	Return A Mass Flow (lbs/hr)	Return B Mass Flow (lbs/hr)	Return B Enthalpy (BTU/lb)	Return A Enthalpy (BTU/lb)	Supply Enthalpy (BTU/lb)	Energy Delivered (BTU/hr)	Energy Input (Watts)	COP
2:30:20 PM	1,743	1,814	20.3	21.7	27.9	24,608	3,426	2.29
2:30:21 PM	1,743	1,814	20.3	21.7	27.9	24,554	3,414	2.29
2:30:22 PM	1,743	1,814	20.3	21.7	27.9	24,559	3,420	2.28
2:30:23 PM	1,743	1,814	20.2	21.7	27.9	24,556	3,408	2.29
2:30:24 PM	1,743	1,814	20.2	21.7	27.9	24,581	3,408	2.29
2:30:25 PM	1,743	1,814	20.2	21.7	27.8	24,531	3,408	2.29
2:30:26 PM	1,743	1,814	20.2	21.7	27.9	24,600	3,402	2.30
2:30:27 PM	1,743	1,814	20.2	21.8	27.9	24,624	3,402	2.30
2:30:28 PM	1,743	1,814	20.2	21.8	27.9	24,598	3,402	2.30
2:30:29 PM	1,743	1,814	20.1	21.8	27.9	24,687	3,402	2.31
2:30:30 PM	1,743	1,814	20.1	21.8	27.9	24,689	3,408	2.30
2:30:31 PM	1,743	1,814	20.1	21.8	27.9	24,653	3,402	2.31
2:30:32 PM	1,743	1,814	20.1	21.8	27.9	24,578	3,402	2.30
2:30:33 PM	1,743	1,814	20.1	21.8	27.9	24,574	3,402	2.30
2:30:34 PM	1,743	1,814	20.1	21.9	27.9	24,665	516	15.22
2:30:35 PM	1,743	1,814	20.1	21.9	27.9	24,748	510	15.45
2:30:36 PM	1,743	1,814	20.1	21.9	27.9	24,668	511	15.36
2:30:37 PM	1,743	1,814	20.1	21.9	27.9	24,561	510	15.31
2:30:38 PM	1,743	1,814	20.1	21.9	27.9	24,654	510	15.37
2:30:39 PM	1,743	1,814	20.1	21.9	27.9	24,587	510	15.33
2:30:40 PM	1,743	1,814	20.1	21.9	27.9	24,691	510	15.39
2:30:41 PM	1,743	1,814	20.1	21.9	27.9	24,627	510	15.35
2:30:42 PM	1,743	1,814	20.1	21.9	27.9	24,737	510	15.42
2:30:43 PM	1,743	1,814	20.1	21.9	27.9	24,703	504	15.58
2:30:44 PM	1,743	1,814	20.1	21.9	27.9	24,633	505	15.52
2:30:45 PM	1,743	1,814	20.1	21.8	27.9	24,592	510	15.33
2:30:46 PM	1,743	1,814	20.1	21.8	27.8	24,556	510	15.31
2:30:47 PM	1,743	1,814	20.1	21.8	27.8	24,433	505	15.39
2:30:48 PM	1,743	1,814	20.1	21.8	27.7	24,265	510	15.13
2:30:49 PM	1,743	1,814	20.1	21.8	27.7	24,133	504	15.22

Note the COP values over 15! Clearly, this is one of the times when the blower remains on extracting residual heat from the coils after the compressor has turned off at 2:30:33. Because this heat is useful and has been paid for, these values must be included. The clarity in this set allows for this as we know we have monitored all of the inputs and outputs carefully. Earlier sets could not guarantee this as they might have simply captured the end of a cycle where energy appeared cheap, when in fact it had been paid for off the record.

7 Results and Concerns

The data taken on one-second intervals is seen as the most important of the study. Having a better grasp over the exact duration of compressor run time provides more accurate work input data, giving a more reliable COP value. The following table shows these values alongside the manufacturer's data. These numbers were calculated based on a filter factor of 65% for System A and 75% for System B. These filter factors were estimated based on observations made during the collection of this data set. The manufacturer's data is based on ARI standard testing which uses 50°F constant temperature groundwater.

Table 4 Short-Cycle COP vs Manufacturer's COP

System	Measured COP	Manufacturer's COP
A	3.44	4.2
B	3.93	4.4

This more reliable data also suggests that System B is more efficient than System A. While System B operates with nearly 89% of the expected performance, System A seems to operate closer to 82%. This section examines this discrepancy, suggesting a number of reasons why this might be the case.

Comparisons between the two geothermal systems show a number of differences. The dominant differences in measurements are the mass flow rates and the geothermal supply water temperature stability.

The mass flow rates are largely dependent on the velocity measurements taken and the "filter factor" used in the calculations. The measurements taken are believed to be consistent and accurate for reasons described above. Over time, however, the velocities in the system will not remain constant. The filter factor is used to account for this and represents a significant unknown. This unknown acts as a counterbalance to the constant-air-velocity assumption.

7.1 Filter Factor

The filter factor was introduced to deal with numerous items which impede or, in some cases, increase the air velocity through the air handler. Return-air filter clogging is likely the most significant of these variables, hence the name of the compensating factor. Other variables may include the opening or closing of doors between the registers and returns, opening or closing of registers, and movement of furniture which may partially block the registers. The filter factor is used as simple multiplier for the volumetric flow rate. The filter factors chosen, based on the nature of the data and the operating conditions seen on site, range from 50% to 90%. The variation in the coefficients of performance as a function of filter factor can be seen in Figure 25. The COPs shown are from the cooling data and the one-second interval data. Neither set is manipulated with respect to outliers.

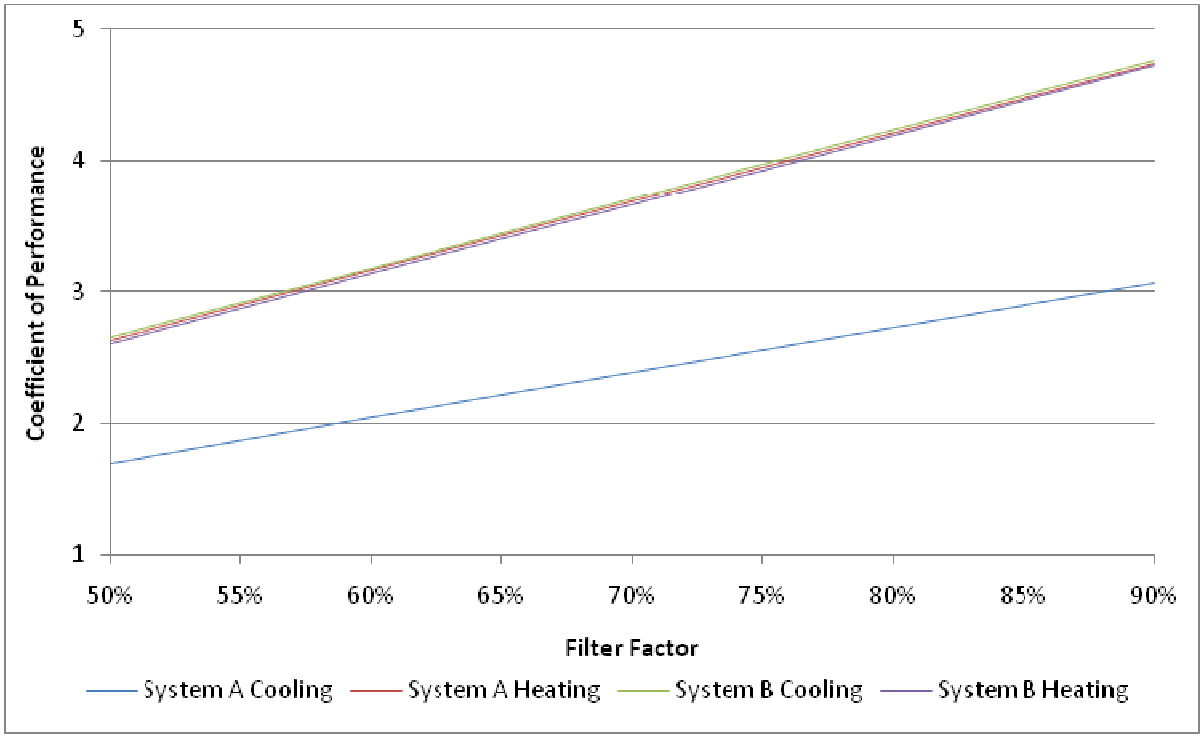

Figure 25 Geothermal COP as a Function of Filter Factor

Surprisingly, the two systems have nearly identical COP trends for their heating cycles, which are essentially the same as the cooling performance trend of System B[ix]. It is believed that the filter factor for System B is higher than that of System A, meaning that the COPs of each system will differ more significantly than the above graph would imply. This is especially believed to be true for the heating data. System B had new filters installed prior to the data collection, causing for a substantially higher filter factor than System A.

It initially appears that keeping a clean filter would ensure higher performance of System A. While this is true, it will not simply translate to the performance indicated in Figure 25. A change in the flow rate of air will be counterbalanced by a reduction in enthalpy difference

across the coils. The heat flow from the air handler will likely not change substantially. Instead the hot air from the air handler will slightly cooler when flowing at a higher rate.

The size of the return registers and the average velocities across them show that system B has a higher mass flow rate at the time of measurement. As $Q = \dot{m} \cdot \Delta h$, this directly affects the coefficient of performance. However, variations in air flow are not the only contributing factor in superior performance of System B.

Although the comparison is not made directly in this study, largely due to a lack of confidence in the transient data from the cooling season, the COP for both systems' cooling cycle is significantly lower than the manufacturer's claims even at 90% filter factor!

7.2 Geothermal Supply Temperatures

As has been noted, geothermal heat pumps take advantage of the stable ground temperatures which are closer to desired conditioned temperatures than outside air. Access to these temperatures is dependent on the method of exchanging heat. Ideally, the temperature of the water coming from the ground, referred to as the geothermal supply temperature, is fairly constant. Variations will occur as these particular systems will not reach steady state. The data strongly suggests that the geothermal supply temperatures for System B are more stable throughout the cycle. These temperatures, along with compressor power, are shown in Figure 26 below.

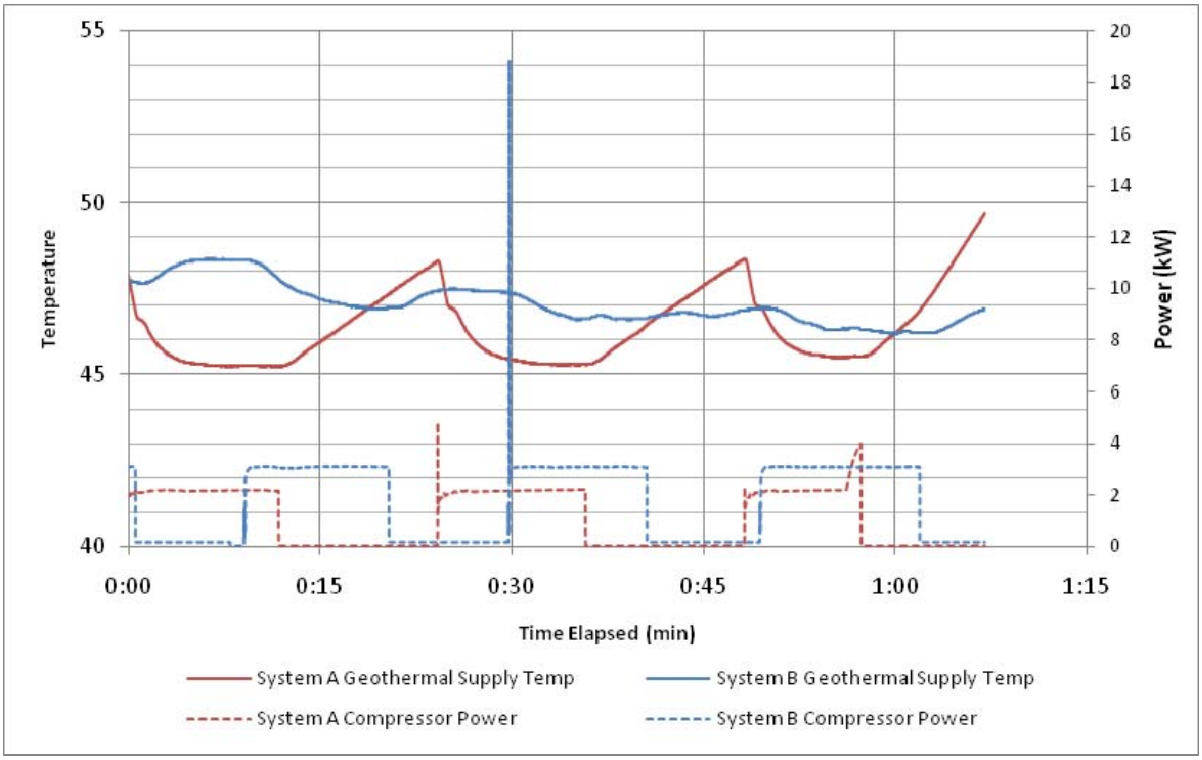

Figure 26 Geothermal Supply Temperatures and Compressor Power

This data was collected on one-second intervals over a one-hour period during the heating season. The correlation between compressor operation and geothermal temperature for each system is clear; when the compressor is running, the geothermal supply temperature is dropping towards a constant temperature. However, it appears as though this asymptotic temperature is changing between the cycles, increasing in the case of System A and decreasing in the case of System B. Temperatures here have been adjusted based on the collection environment. The air handler for System A is in conditioned space while the air handler for System B is located in an unconditioned area beneath the house. Temperatures have been lowered by 5 °F in the System A data and have been raised 3 °F in System B to account for heat transfer with the environment. It is believed that, from this data and other sets taken over the course of the study, the geothermal heat exchange system for System B is superior to that of System A. This contributes to the higher coefficient of performance of System B, as condenser temperatures are lower in the summer and evaporator temperatures are higher in the winter. Given the hybrid nature of System B, having a groundwater and surface-water heat exchanger, this is not surprising. However, the reinjection scheme for each system is not known. It is possible that the reinjection water for System A interacts with the groundwater being removed for the heat pump. The interaction will certainly affect the performance of the heat pump as the groundwater drawn into the system will be colder in the winter and warmer in the summer; not a desirable effect.

7.3 Geology

The two systems lie in different areas geologically. Geology has a strong impact on system performance in groundwater systems. Since open groundwater systems tend to exchange heat mostly through convection, the flow rates of the groundwater in the geological formation have a significant impact on the overall heat transfer of the system. Figure 27 shows the differing geology surrounding System A and System B. On the following page, Figure 28 shows the geological variation throughout the state, including the key for these maps (NC Geological Survey, 1991). The variation in the maps, along with the varying heat transfer and heat capacity properties of the underlying rock listed in Table 5, show the importance of having a strong understanding of the geology of a region in sizing a geothermal heat exchange system (Banks, 2008; Ugur, 2006).

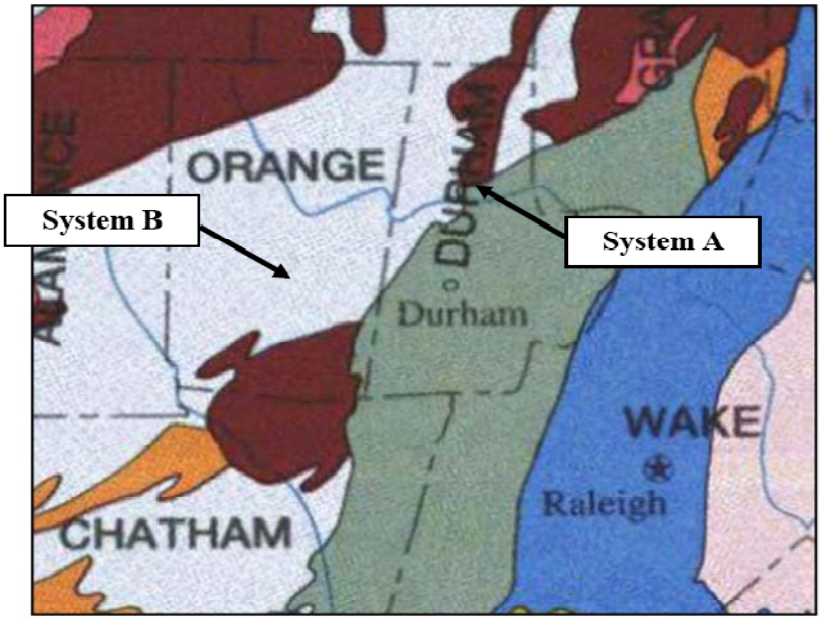

Figure 27 Local Geology

Table 5 Hydraulic and Thermal Properties of Local Rock Types

Formation Type	Hydraulic Conductivity (m/s)	Thermal Conductivity (W/m·K)	Volumetric Heat Capacity ($MJ/m^3 \cdot K$)
Metamorphosed Granitic Rock	Depends largely on fracturing Without fracturing - impervious	3.0 – 4.0	1.6 – 3.1
Sandstone	10^{-9} to 10^{-4}	2.0 – 6.5	2.0 – 2.1
Slate	10^{-12} to 10^{-9}	2.54	-

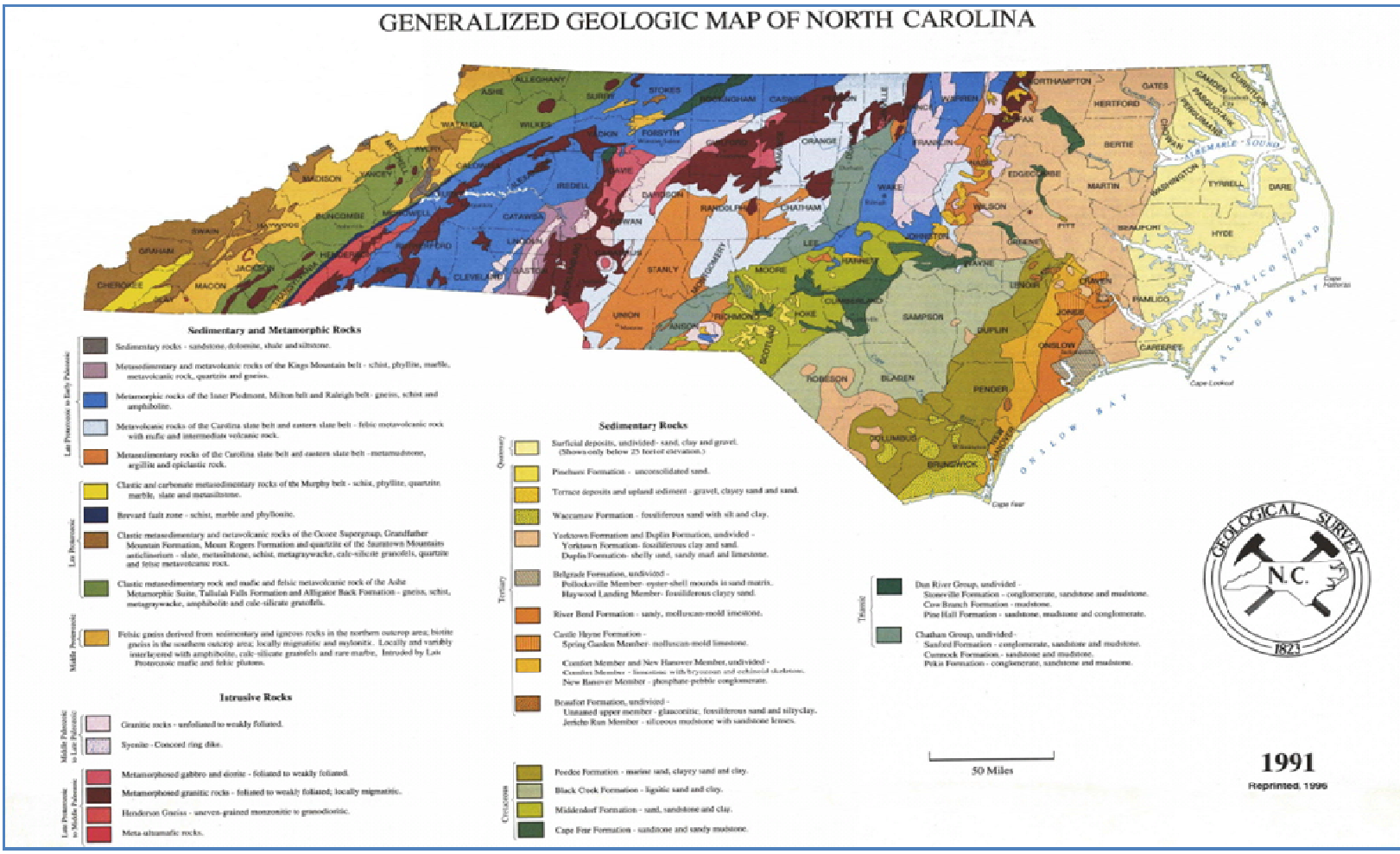

Figure 28 Geology of North Carolina

From Figure 27 it is clear that System B is located within a metavolcanic slate belt: a mixture of *"felsic metavolcanic rock with mafic and intermediate volcanic rock"*. The geology of System A is a bit less obvious, as the system seems to be located on a boundary between metamorphosed granitic rock and the Chatham Group: mostly a combination of conglomerate, sandstone, and mudstone. It is likely that the geologic differences here have an impact on system performance, as the groundwater flow rates will vary between these two areas.

Given the lower performance of System A, it is possible that the reinjection methods were designed properly, but the groundwater flow through the aquifer is more restricted than in the slate rock of System B. If this is the case, it would seem that System A likely extracts water from an aquifer lying in the Chatham Group. These more sedimentary rocks are porous than those in the slate belt, however igneous and metamorphic rocks have the ability to structurally support fissures in the aquifer. This often allows higher flow rates of the groundwater and thus higher heat transfer[x].

It is also possible that groundwater flow was not understood fully in designing the abstraction and reinjection practices for System A. It could be that the abstraction and reinjection wells are one and the same. This would cause for high levels of thermal interaction within the well. However, in the case that these are not the same, it is highly possible that there are opportunities for thermal interactions in the aquifer. A reinjection well may occur at a significant distance from the abstraction well and still have a high thermal interaction with the abstraction well. This is especially true in volcanic and metamorphic rock where fissures

may allow for high flow between the two wells. In this scenario, it is quite possible that System A lies on top of metamorphosed granitic rock rather than the Chatham Group, where stress fractures may allow for high hydraulic conductivity from the reinjection region to the abstraction region. These interactions can quickly compromise the efficiency of a geothermal system. Observations made during site visits suggest that the area lies in a more granite rich area.

Many aspects of hydrology are important for designing a proper open geothermal system. Hydraulic conductivity is appropriately analogous to thermal conductivity[xi]

The system's installer was contacted and questioned regarding the testing methods for determining the heat transfer properties of the aquifer and underlying rock. Unfortunately, the installer was unresponsive.

7.4 Fan Power

It is possible that the fan power data from system B was not accurate. From Figure 23 the fan power for System B appears to be around 85 watts. An 85-watt fan is equivalent to just over $1/10^{th}$ hp. This is energy input and it is likely that a motor this small has an efficiency of only 50%. Therefore the power output from the motor is near $1/20^{th}$ hp; far too small for this system. This is smaller than the rated hp of the blower motor. The reasoning for this error is not known. All electrical inputs were monitored, wires were traced to the blower, and blower voltage was measured, further supporting that the fan was powered by the only 120 volt cable entering the system. It is possible that the CT used read the data improperly. This may also contribute to the higher COP of System B.

7.5 Cycle Lengths

The short cycle heating data shows that the cycle time for System B is less than that of System A. This not only produces a higher instance of transience with respect to compressor power, as mentioned on page 48, but also increases the amount of time when the air flow is beginning and ending. These periods of less than maximum air flow rates will result in a higher COP as the heating or cooling delivered from the air handler is directly proportional to the air mass flow rate.

7.6 Ideal COPs

Interestingly, the results from the ideal COP calculations show System A as having a higher Carnot efficiency than System B. These calculations are based on the equations shown on pages 10. Temperatures were converted to the thermodynamic scale (Rankine) and heat exchanger approaches were assumed. A heat exchanger approach represents the temperature difference, on average, between the two fluids exchanging heat. For example, the air handler coil approach assumed was 5°F. This means that during the heating mode, the air leaving the heating coils is 5°F cooler than the coils themselves. In any heat exchanger the overall average temperature of the fluid receiving heat must be lower than the one releasing heat, as dictated by both our experience and the 2nd Law of Thermodynamics.

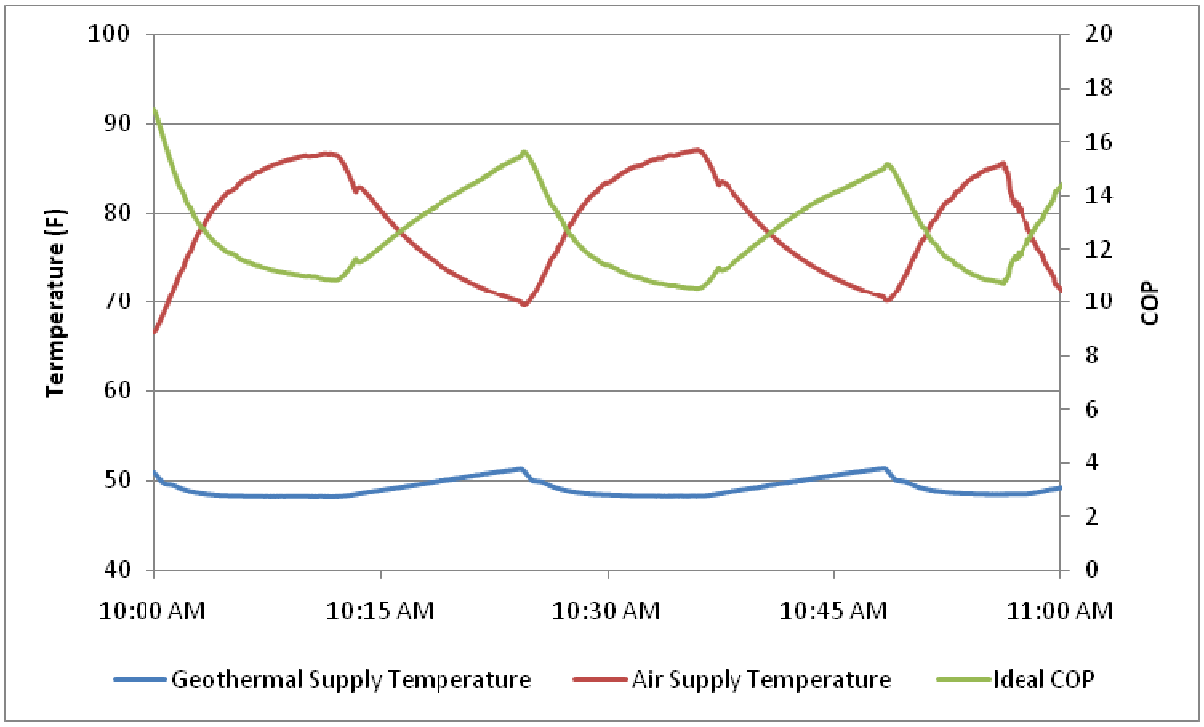

Figure 29 System A: Carnot Efficiencies with Heat Exchanger Temperatures

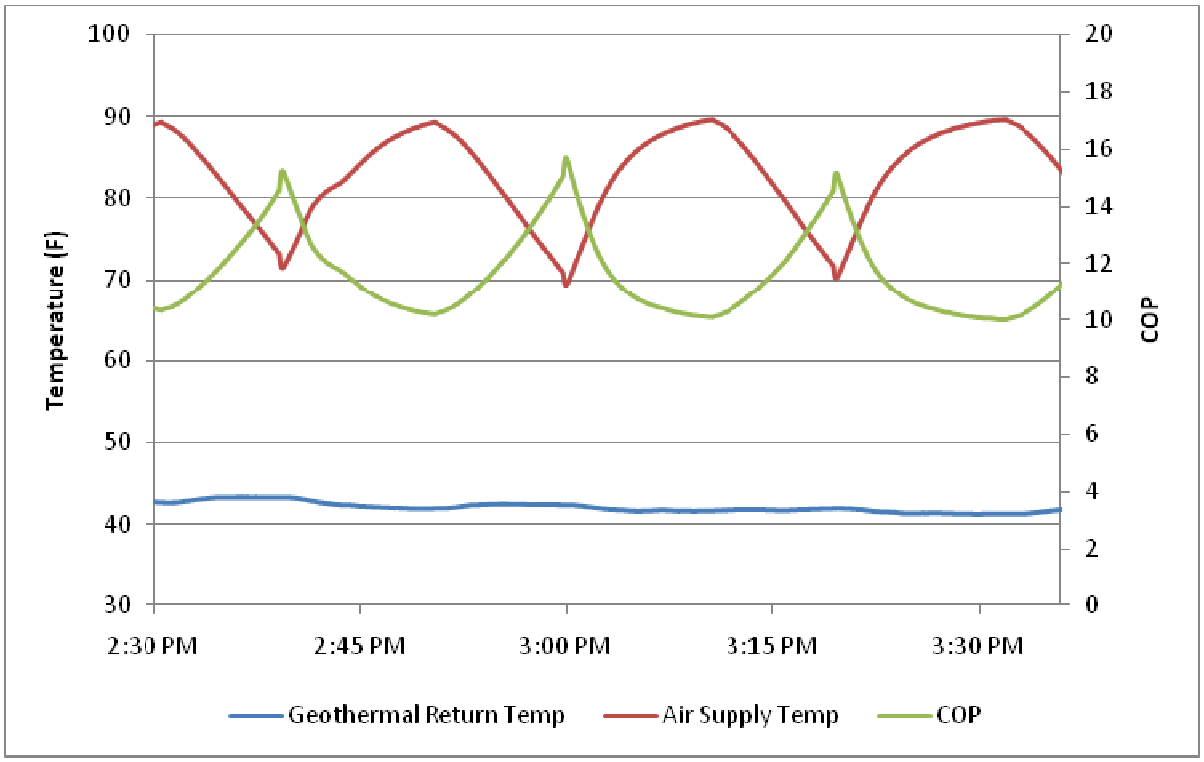

Figure 30 System B: Carnot Efficiencies with Heat Exchanger Temperatures

The data above is based on a 5 degree approach on the heating coils and a 2 degree approach on the geothermal heat exchanger. While the geothermal approach should be based on the temperature leaving the heat exchanger as well as the temperature being supplied, one of the thermisters from System B showed signs of faulty data. Initially the average of the supply and return temperatures from the geothermal heat exchanger was going to be used, but given the faulty data and the fact that this data is only used to find a general trend, the supply temperature (going to the heat pump from the ground) alone was used.

From these calculations the average ideal COP for System A is 12.7 and the average ideal COP for System B is 11.6. This is somewhat surprising given the results from the actual COP calculations. However, ideal COPs neglect many important variables, several of which

are listed on page 11 in the “Real Heat Pumps” section. It is possible that System A shows better performance, in terms of ideal efficiencies, because of the seemingly higher geothermal supply temperatures. The exact temperature of the geothermal water is not known; measurements were taken from the brass inlet and outlet water fittings.

On page 61, following Figure 26, it is explained that the temperatures of the geothermal supply water were lowered 5 degrees for System A and raised 3 degrees for System B. This was an estimate initially made because of the temperatures of the surrounding air; System A is located in conditioned space while System B is not. However, it was later realized that this would most likely be the case when the geothermal loop is not flowing. The thermisters were insulated and strapped to brass fittings. When the geothermal loop is flowing the convective heat gain from the conditioned space should not have a significant effect. For this reason, the adjustments to the geothermal supply temperatures were not made in calculating the Carnot efficiencies.

8 Economics of System A

A valuable opportunity was presented when the owner of System A conveyed that historical data for the electrical billing for the house was available. The data spans nearly four years. The geothermal system was installed about half-way through this data. This section explores the trends in this data.

Despite the lower COP of System A, which was notably less expensive to install, the heating and cooling costs have been reduced significantly. Figure 31 shows the costs and energy use of System A. Energy use data was only available after the system was installed. The homeowner did not collect energy usage data prior to this. However, since the vast majority of the electrical charges are for energy, a clear trend is evident in Figure 31 on the following page.

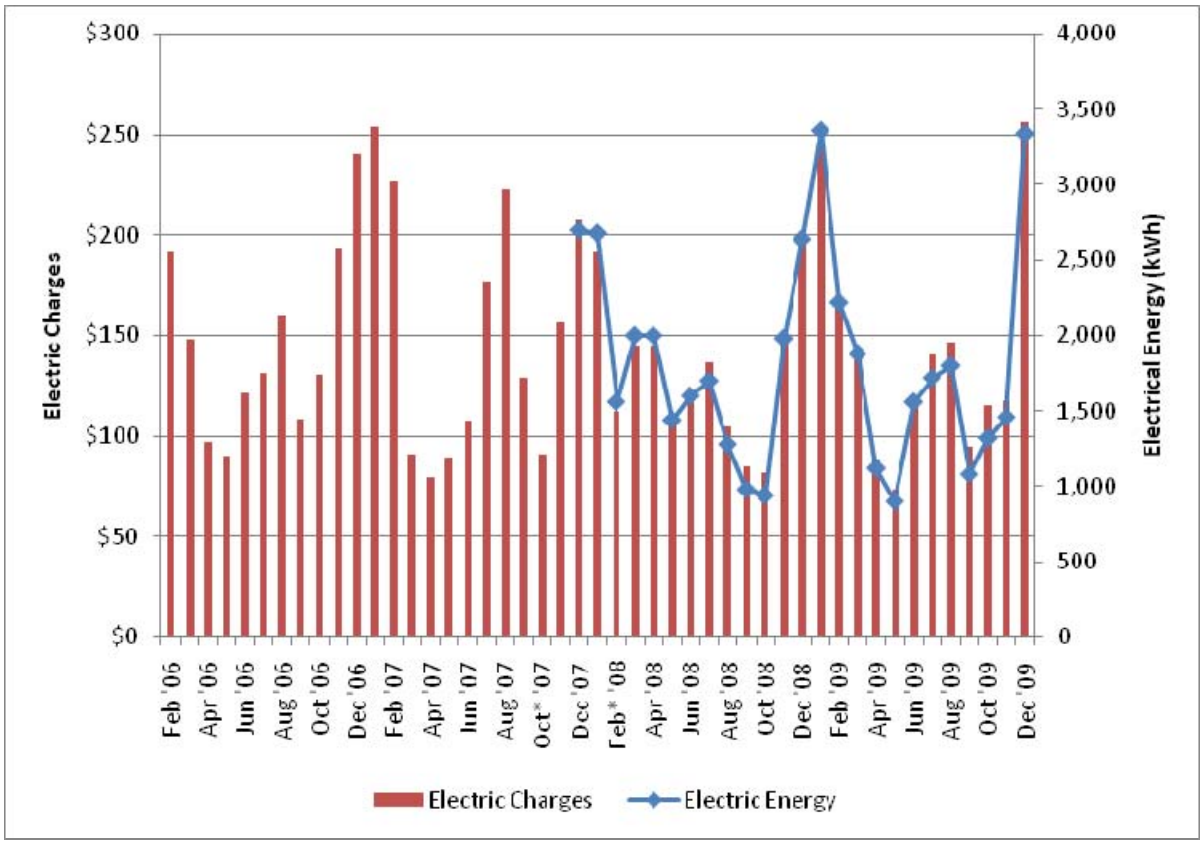

Figure 31 System A: Electric Costs and Use

By the figure, it does not appear that the bills have been reduced much from before the geothermal system was installed in October 2007[1]. However, comparing heating and cooling costs is not as simple as comparing bills due to fluctuations in the heating and cooling loads over the years.

To compensate for this variation, heating and cooling degree days are used. The heating degree day is a unit of the product of time and temperature difference; one heating degree day can represent 24 hours where the outside air temperature is one degree lower than the

[1]The system was initially installed in October of 2007, but problems with improper sizing resulted in having a larger system installed in February of the following year. Both months are noted with an asterisk in the figures.

indoor air temperature. One heating degree day can also represent one hour where the outside air temperature is 24 degrees lower than the inside air temperature. Similarly, cooling degree days represent periods where the outdoor air temperature is higher than the desired temperature in the conditioned space.

Figure 32 displays the variation in heating and cooling loads from year to year. Heating and cooling degree days are generally representative of system loads, but loads will also vary because of changes in internal heat generation, occupancy, and, during the summer, humidity levels outdoors. The cooling required for condensing water vapor out of the air in the summer is a significant portion of the cooling load and is not distinctly represented in cooling degree days.

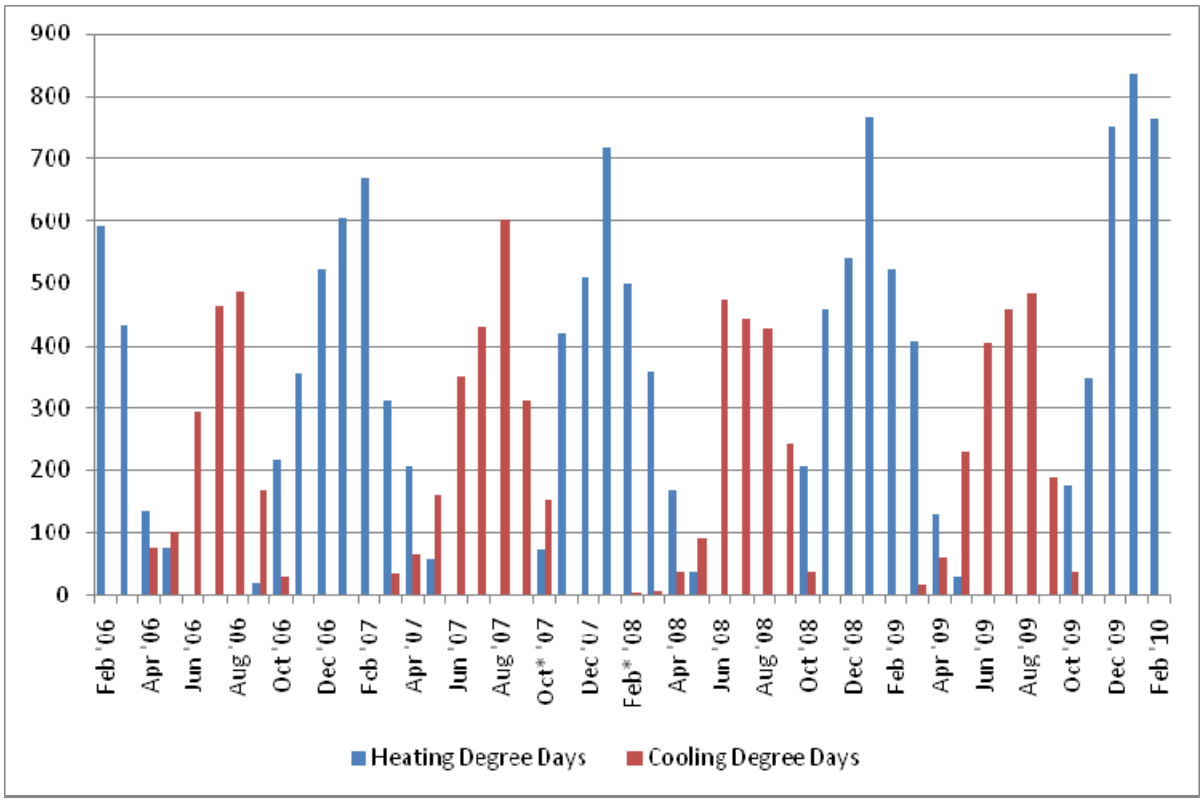

Figure 32 System A: Heating and Cooling Degree Days

This data will need to be adjusted as only a portion of the energy use in the home is for space conditioning. In January, for example, the portion of the utilities which are used for space heating is quite different from the portion used for heating in July[xii]. The method for adjusting the billing information to account for this is outlined in Appendix E. The trend in Figure 33 is believed to be representative of the changing cost of extreme weather. This figure shows an overall subtle decline in the cost of both heating and cooling degree days after October '07.

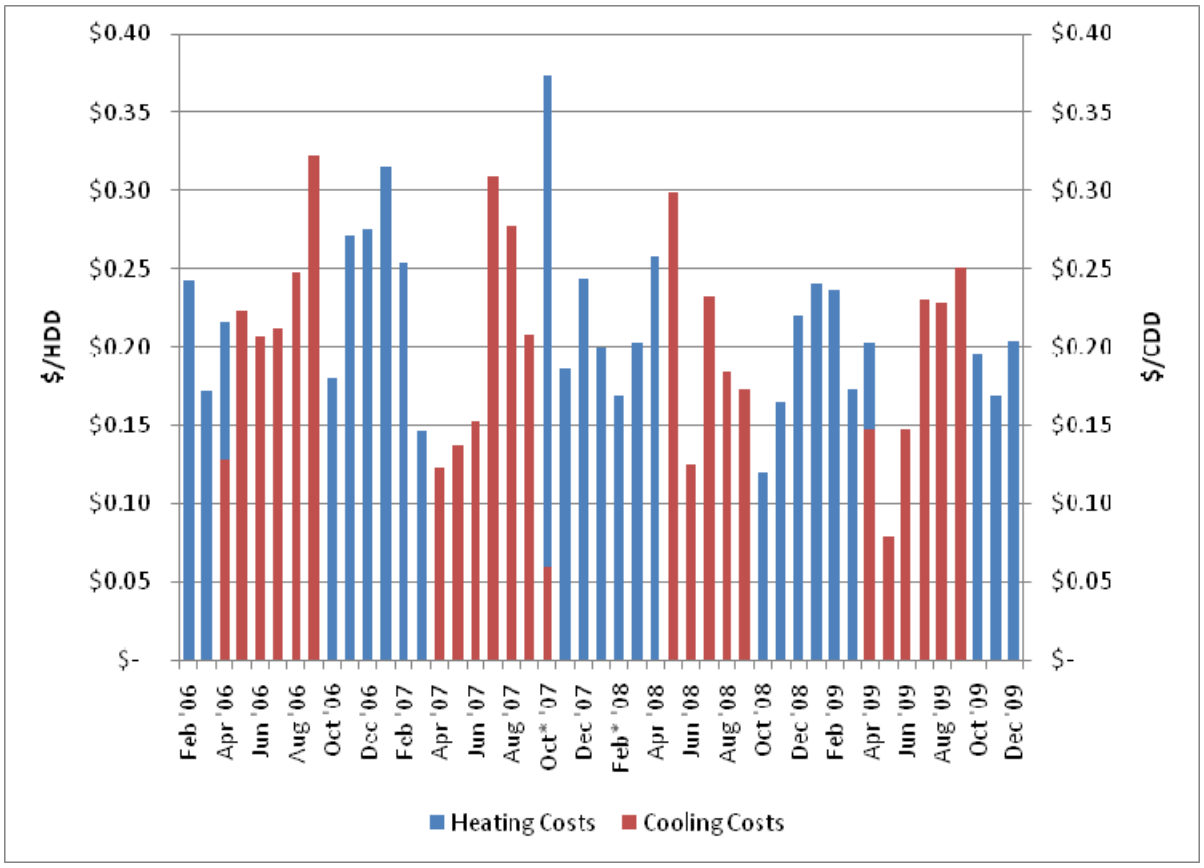

Figure 33 System A: Cooling and Heating Cost per Degree Day

Average costs for heating and cooling degree days were calculated to further quantify the change. These averages are shown in Table 6.

Table 6 Average Cost for Heating and Cooling Degree Days

System A	Average $/HDD	Average $/CDD
Before Geothermal	$0.219	$0.212
After Geothermal	$0.200	$0.190

This shows an operating cost reduction of 9.5% in the winter and 11.6% in the summer. It is important to note that these numbers are approximate and based on assumed percentages of the electrical energy going to space conditioning, depending on the time of year.

9 Conclusions and Future Work

Geothermal heat pump systems have proved themselves to be a viable technology. However, this is only when they are properly designed and constructed. The purpose of this research was to attempt to determine the actual performance of two geothermal heat pumps in the field. **The systems operated at between 11% and 18% less efficient than manufacturer's claim in the heating cycle.** These values are believed to be fairly accurate because of the resolution of the data logging equipment. **The variation in the calculated heat-pump performance is too great to be conclusive.** The highly variable nature of the cooling data efficiencies is believed to stem from the logger intervals primarily.

It is clear that air velocities, transient behavior, and logger errors posed significant hurdles to achieving accurate results. However, it is believed that the data and analytical methods used are valid for such systems. There will always be room for improvement though. **These primary areas of concern could be improved by the following**:

1) **Air velocities –** In order to overcome the variation in air velocities, future work would have these monitored as well, using pressures sensors in the air handler. The pressure readings and shaft power input could then be correlated to air flow rates using the blower curve, eliminating the need for the assumptive filter factor.
2) **Transience –** This problem is solved by the same method used in this research: shorter time intervals for the data collection. While long term behavior is valuable in understanding the general trend of the system's operation, short interval data is far more valuable in determining operating efficiencies in system which do not operate in

quasi steady state conditions. Future work would take far more data using higher resolution logging intervals.

3) **Logger Errors –** It is difficult to know exactly how to handle this issue without simply using more than one logger for each parameter. The use of multiple loggers presents a fail-safe to suspect data. Collecting multiple sets of the same data increases the confidence of the study. An additional way to confirm measurements, used in this study on numerous occasions, is to take measurements using additional equipment at specific times when the data loggers are collecting data. In both geothermal systems amperage data was collected using an ammeter at a specific time. This data was then compared to the data reading from the logger at that same point in time. This could be carried out for several variables, however it only shows validity for that particular moment.

In addition to these means of solving some of the concerns of the project, it would be valuable to explore data acquisition in general further. Many systems have monitoring units built into controls. Several geothermal monitoring systems were investigated. Of the units found, few sampled temperature data points more frequently than every minute! It seems as though the desire for monitoring was not to ensure efficient operation, but rather operation itself.

An interesting future project would be to set up a monitoring system which had capabilities to collect and store large amounts of data. Monitoring and storing data using intervals of less than 5 seconds could provide highly realistic and valuable data.

In addition to these concerns and ideas for improvement, **it would be an excellent opportunity to incorporate two air-to-air heat pumps into the study fully**. System C, as has been mentioned, was not used extensively for several reasons. The data from this system is found in Appendix E.

This study shows the lack of performance of geothermal heat pumps in comparison to the optimized data from the manufacturer, but how does an air-to-air heat pump truly compare? **It is quite possible that an air-to-air heat pump is also far less efficient than their manufacturers claim.** For example, air-to-air heat pumps operate in a defrost cycle when ice builds up on the outdoor coils. This is typically accomplished by the use of electric strip heat. As has been mentioned, this form of heat is detrimental to heat pump efficiency. These cycles are not always accounted for in manufacturer's data on heat pumps.

It is difficult to compare the two types of system without having data collected using the same methods and similar operating conditions. I am almost certain that any manufacturer's data will not have been gathered using the "in field" methods used in this study. Because of this, I would not be any more likely to recommend an air-to-air heat pump than I was prior to the study. In fact, the performance of System B has only been encouraging. **To meet nearly 90% of the manufacturer's characteristically optimistic claims, as System B did, is certainly seen as successful.**

REFERENCES

ASHRAE. (2009). *ASHRAE Fundamentals.* Atlanta, GA: ASHRAE.

Banks, D. (2008). *An Introduction to Thermogeology: Ground Source Heating and Cooling.* Oxford, UK: Blackwell Publishing.

Brodowicz, K., & Dyakowski, T. (1993). *Heat Pumps.* Oxford: Butterworth-Heinemann, Ltd.

Cengel, Y. A., & Boles, M. A. (2008). *Thermodynamics: An Engineering Approach.* New York, NY: The McGraw-Hill Companies.

Dincer, I. (2003). *Refrigeration Systems and Applications.* West Sussex, England: John Wiley & Sons.

DOE. (2006, 11 1). Retrieved January 20, 2010, from A History of Geothermal Energy in the United States: http://www1.eere.energy.gov/geothermal/history.html

FHP. (2009). *Residential Product Guide.* Retrieved January 10, 2010, from Florida Heat Pump: http://fhp-mfg.com/

Geo4VA. (2006). *Geothermal Heat Pump Technology*. Retrieved February 16, 2010, from Geo4VA: http://www.geo4va.vt.edu/indexA.htm

Heap, R. (1979). *Heat Pumps.* London: E. & F. N. Spon Ltd.

Lund, J. W. (2004). 100 Years of Geothermal Power Production. *GHC Bulletin* , 11-19. NC Geological Survey. (1991).

OED. (1989). *geo-*. Retrieved January 19, 2010, from Oxford English Dictionary: http://dictionary.oed.com/

Radermacher, R., & Hwang, Y. (2005). *Vapor Compression Heat Pumps with Refrigerant Mixtures.* Boca Raton, FL: Taylor & Francis.

Ugur, S. D. (2006). Investigation of the relation between the specific heat capacity and material properties of some natural building and facing stones. *International Journal of Rock Mechanics and Mining Sciences* , 831-835.

APPENDICES

Appendix A: Air Velocity Matrices

All measurements were taken in unit of feet per minute. Measurements were tested against data collected from a different type of air velocity meter. The results from these comparisons differed by less than 4%. The data in the following tables are from the hot-wire anemometer. These represent velocities prior to applying the filter factor.

System A:

System A: 16” x 20” Return Duct Velocities

214	223	216
215	228	225
248	312	252
236	300	274

The average velocity for this duct is 245 ft/min

System A: 20” x 20” Return Duct Velocities

240	199	158
161	154	142
174	180	150

The average velocity for this duct is 173 ft/min

System B

System B: 14" x 14" Return Duct Velocities

397	371	341
366	333	380
418	360	417

The average velocity for this duct is 376 ft/min

System B: 20” x 20” Return Duct Velocities

189	195	203
207	155	208
170	195	195

The average velocity for this duct is 191 ft/min

System C

Air velocities measurements on System C were taken before and after a new filter was installed. Below are results for each. In calculations, the new filter data was used, having the filter factor adjust the data for any filter clogging or other factors. The average velocity used was 293 ft/min.

System C: 20" x 20" Return Duct Velocities with Clean Filter

206	200	210
355	333	278
372	342	340

System C: Return Duct Air Velocities with Dirty Filter

214	234	200
300	250	220
341	252	254

Appendix B: Psychometric Calculations

By equation 1.2 (6) of the ASHRAE Fundamentals, the saturation pressure, p_{ws}, of liquid water from 32°F to 392°F can be calculated as

$$p_{ws} = e^{\left(\frac{C_1}{T}+C_2+C_3 \cdot T+C_4 \cdot T^2+C_5 \cdot T^3+C_6 \cdot \ln T\right)}$$

Where,

$$C_1 = -1.0040397\ x\ 10^4$$

$$C_2 = -1.1294650\ x\ 10^1$$

$$C_3 = -2.7022355\ x\ 10^{-2}$$

$$C_4 = 1.2890360\ x\ 10^{-5}$$

$$C_5 = -2.4780681\ x\ 10^{-9}$$

$$C_6 = 6.5459673\ x\ 10^0$$

And,

$$p_{ws} = saturation\ pressure, psia$$

$$T = absolute\ temperature, °R = °F + 459.67$$

This calculation represents an approximation with very high accuracy. The saturated vapor pressure and the saturation pressure of liquid water are negligibly different (ASHRAE,

2009). From the calculated saturation pressure and the relative humidity, φ, the vapor pressure of the sampled air, p_v, can be calculated as

$$p_v = p_{ws} \cdot \varphi$$

The specific humidity, W, is the ratio of the mass of water vapor to the mass of dry air.

$$W = \frac{M_v}{M_{da}}$$

This is equal to the mole ratio, $\frac{x_v}{x_{da}}$, times the ratio of molar masses. The molar mass of water is equal to 18.015268 g/mol and the molar mass of dry air, given the constituents of air and their respective molar masses, is equal to 28.966 g/mol. Therefore

$$W = \frac{18.015268}{28.966} \cdot \frac{x_v}{x_{da}} = 0.621945 \cdot \frac{x_v}{x_{da}}$$

By Dalton's Law, it is known that in a mixture of gases the partial pressure of each compound is equal to the mole fraction of the respective compound in the mix. This tells us that the specific humidity can also be calculated as

$$W = 0.621945 \cdot \frac{\frac{p_v}{P}}{\frac{p_{da}}{P}} = 0.621945 \cdot \frac{p_v}{p_{da}}$$

Where

$$p_{da} = Partial\ Pressure\ of\ Dry\ Air$$

$$P = Total\ Air\ Pressure = 14.696\ psia, constant$$

Given that the dry air and the water vapor are the only constituents of this mixture, the total air pressure is the sum of the partial pressures of dry air and water vapor. This gives absolute humidity as a function of vapor pressure alone.

$$W = 0.621945 \cdot \frac{p_v}{P - p_v}$$

The specific volume, v (the reciprocal of density, ρ) ,and enthalpy, h, of the air samples can now be calculated by equations 1.12 (28) and 1.13 (32) of the ASHRAE Fundamentals Handbook:

$$v = \frac{R_{da} \cdot T \cdot (1 + 1.607858 \cdot W)}{P}$$

And

$$h = 0.24 \cdot t + W \cdot (1{,}061 + 0.444 \cdot t)$$

Where

$$R_{da} = Gas\ Constant\ for\ Dry\ Air = 53.350\ \frac{ft \cdot lb_f}{lb_{da} \cdot °R}$$

$$t = Temperature, °\mathrm{F}$$

Air mass flow rates and air enthalpies can now be calculated.

Appendix C: Additional Calculations

Mass flow rates were calculated as described on page 28 based again on the assumption that air velocities were constant during periods when the supply enthalpy was higher than both the return enthalpies (for heating data). Energy delivered was calculated as

$$Q = \dot{m}_A \cdot \left(h_{supply} - h_{Return\ A}\right) + \dot{m}_B \cdot \left(h_{supply} - h_{Return\ B}\right)$$

Where

$Q = Heat\ Delivered$

$\dot{m}_A = Return\ A\ Mass\ Flow\ Rate$

$\dot{m}_B = Return\ B\ Mass\ Flow\ Rate$

$h_{supply} = Supply\ Air\ Enthalpy$

$h_{Return\ A} = Return\ A\ Air\ Enthalpy$

$h_{Return\ B} = Return\ B\ Air\ Enthalpy$

In the data sets with electric strip heat, this heat was converted from kW to BTU/hr and added to Q. This was done because of the location of the strip heating elements downstream from the air supply data logger, as can be seen in Figure 7 on page 24.

Energy input was calculated as the sum of all power run into the system. The electrical input data which was logged was calculated as described on page 25. Power for the other components, such as the geothermal water pump, was added in based on nameplate data.

The COP values were calculated as the ratio of heat delivered to work input multiplied by the conversion factor 3.413 BTU/Wh.

Appendix D: Corresponding Data Figures

Each figure in the data section of this paper has a corresponding figure for each of the other two systems. Several of the sections only use one of the pairs of graphs, either the System A graph or the System B graph. For example, Figure 12 in the data section shows the air supply conditions and the compressor power for System A during the cooling season. In this Appendix, the air supply conditions and compressor power for Systems B and C are shown following the reference to Figure 12, as shown below. This is carried out for all single figures in the data section.

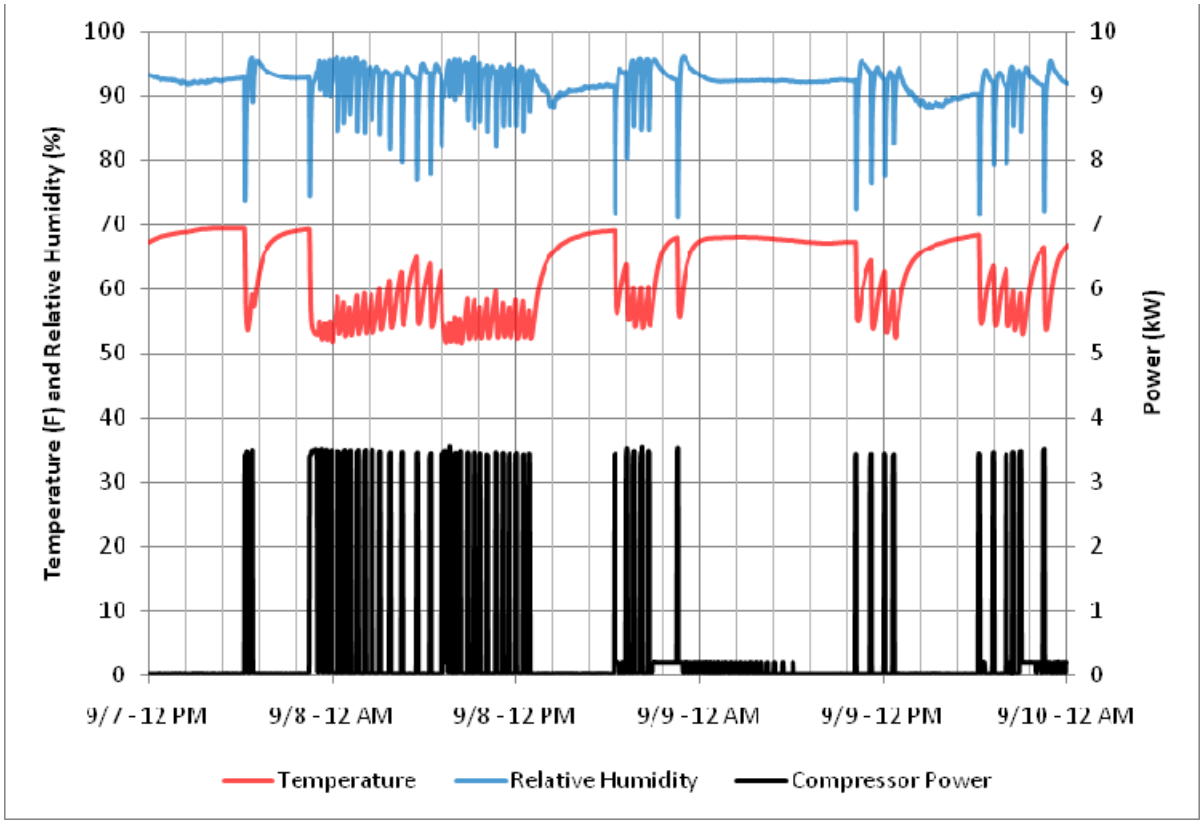

Figure 34 System B: Air Supply Conditions and Compressor Power - Cooling Season

Note the power scale in comparison to Figure 12. System B has higher power consumption in the compressor by nearly 75%. The higher COP of System B is likely a result of the higher air flow rates across the conditioning coils.

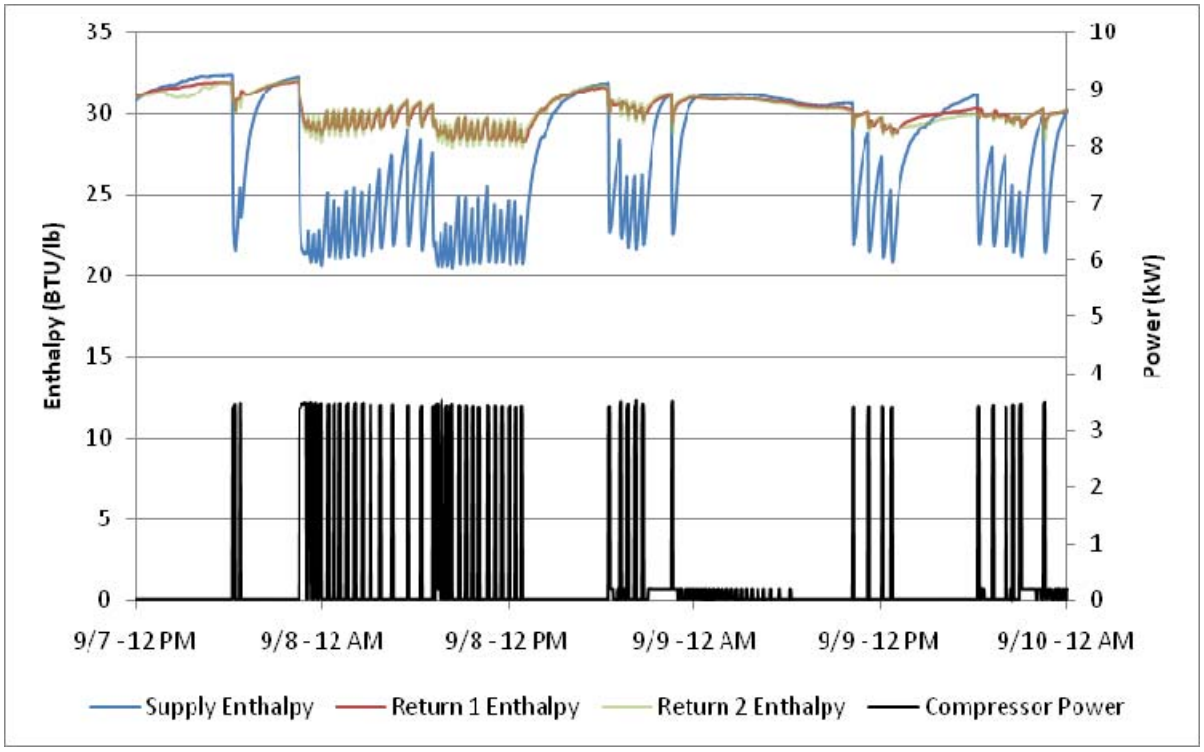

Figure 35 System B: Air Enthalpies and Compressor Power - Cooling Season

This graph follows Figure 13 in that the enthalpy of the supply is dropped significantly while the compressor is running, as expected. The oscillations in supply and return enthalpies are believed to simply be the rising and lowering of enthalpies between and during cycles respectively.

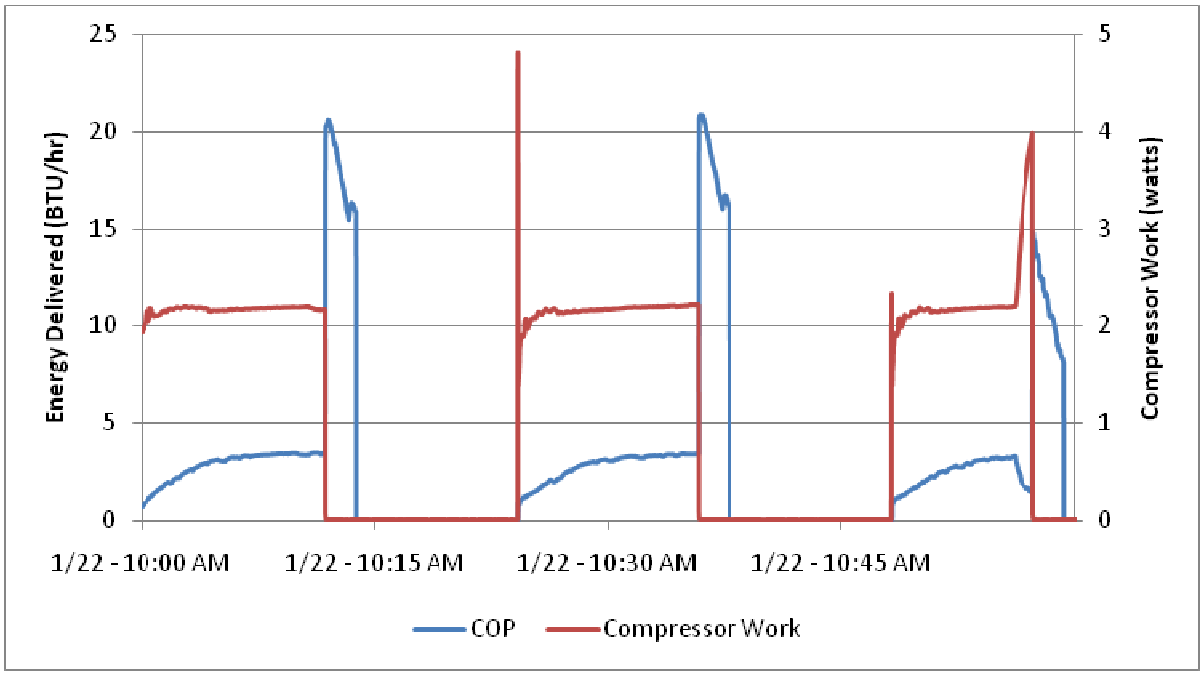

Figure 36 System A: Short Cycle COP and Compressor Power

Figure 36 corresponds to Figure 23. The data from the fan power was not read during this cycle. It is not known why this was the case. This is the reason energy calculations were then based on enthalpy differences rather than system power.

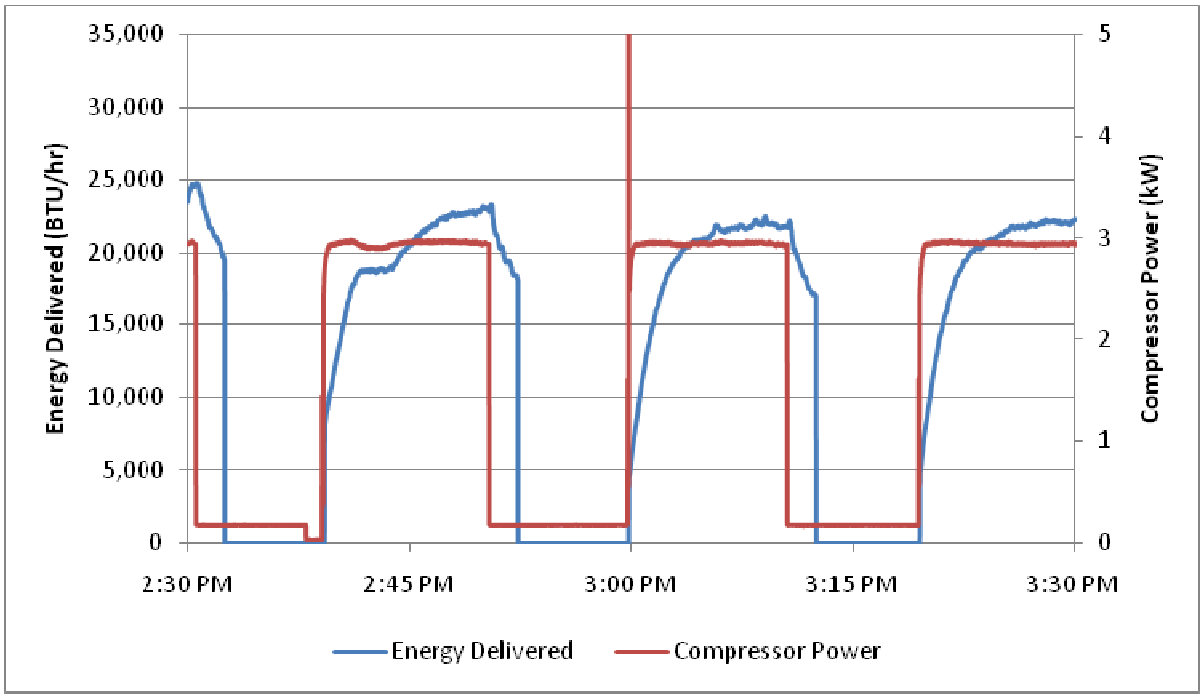

Figure 37 System B: Energy Delivered and Compressor Power

Figure 37 corresponds to Figure 24 from the short-interval data set.

Appendix E: System C Data

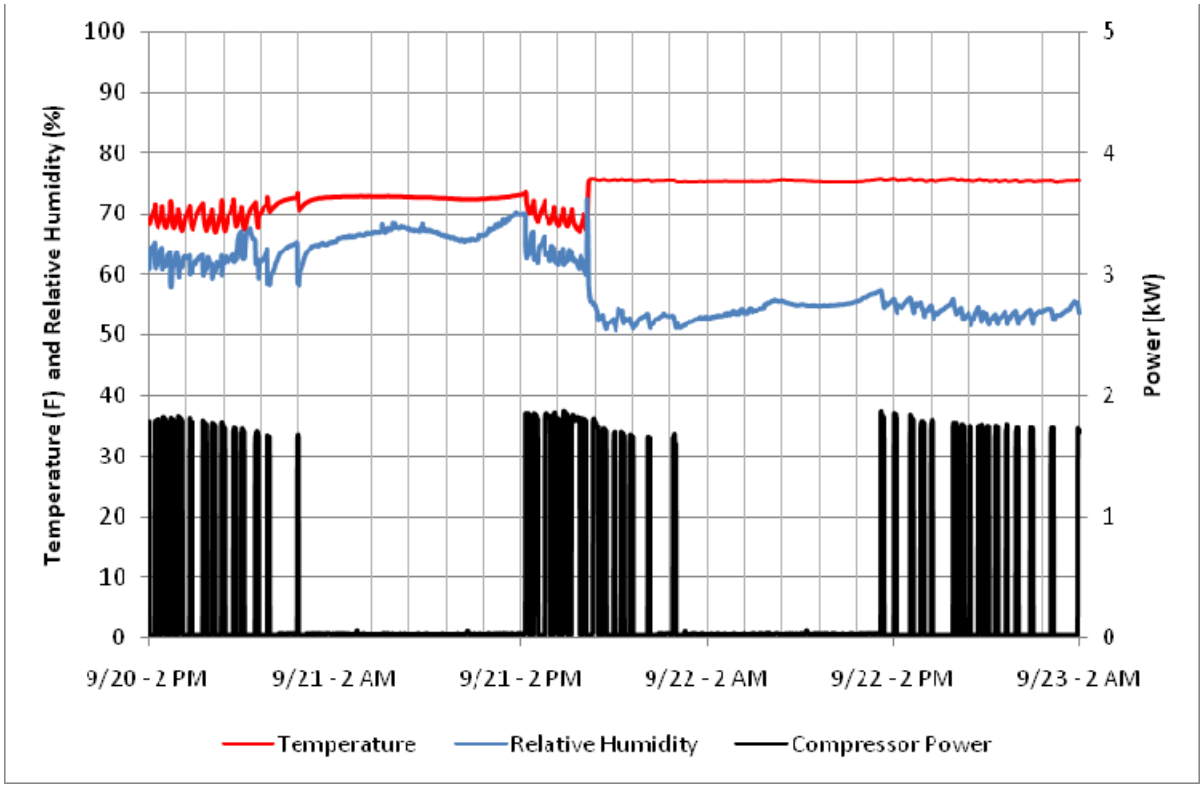

Figure 38 System C: Supply Conditions and Compressor Power - Attempted Cooling Season

This data set clearly did not capture the cooling season. The data above is suspect given the fact that compressor operation having the same effect on the relative humidity and temperature initially. The lack of any noticeable effect on the temperature after later in the evening on 9/21 also strongly suggests the data is corrupt. Neither of these phenomenons should be occurring. They are attributed to a faulty data logger.

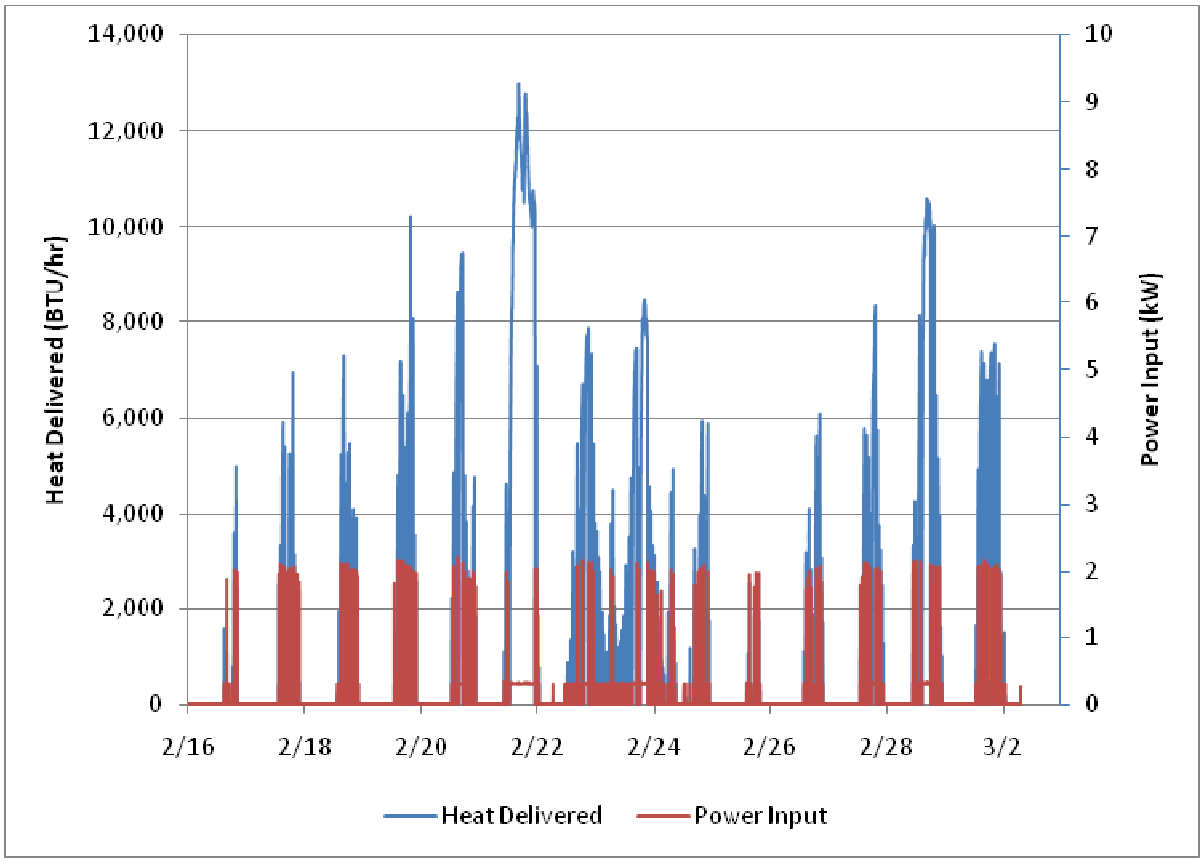

Figure 39 System C: Heat Delivered vs Power Input

This data also shows suspecting behavior. The periods of highest heat delivery required minimal power. It is possible that this is resulting from electric strip heat which was believed to be monitored. These periods of high amounts of low-cost heat are believed to be due to either faulty data logger behavior or a lack of heat strip monitoring. However, these points would create very high COP values. When these points are eliminated the COP drops from 5.41 to 4.55. This reduction of only 16% is far too small. 4.55 is still an unreasonable COP for a typical air-to-air unit. This behavior in the data led to the belief that this data was unreliable and therefore not used.

Appendix F: Calculations for System A Electrical Energy Billing

As mentioned, the percentage of the energy bill which goes towards space conditioning will vary throughout the year. The following percentages were assumed for the amount which went to billing. Their values are arbitrary and since these percentages are being used throughout the entire period, they will show how the trend changes as the geothermal system is brought online.

Estimated Space-Conditioning Cost Percentages

Month	Heating %	Cooling %
January	75%	0%
February	75%	0%
March	50%	0%
April	30%	10%
May	0%	25%
June	0%	50%
July	0%	75%
August	0%	75%
September	10%	50%
October	30%	10%
November	50%	0%
December	60%	0%

From these percentages, the cost per heating degree day was calculated by first establishing whether or not the number of heating degree days was sufficient to have a serious impact on the bills, or even turn the system on for that matter. If only 50 or less heating degree days occurred during the month, it was assumed that the system did not come on (likely due to the

thermal mass of the home being able to sustain desirable conditions for brief periods of cold weather). If the outside conditions resulted in more heating degree days, then the monthly energy bills were multiplied by the percentage of the bills used for space conditioning and divided by the number of heating degree days for that month.

Cooling degree day costs were calculated using the same method.

END NOTES

[i] While other cycles, such as absorbtion and adsorbtion cycles, are also capable of pumping heat, these cycles are not investigated here.

[ii] Other criteria include reactivity (corrosion), flammability, toxicity, and cost. These affect the long term economics and safety of the refrigerant, but do not the immediate mechanics of the heat pump.

[iii] In fact, this theoretical maximum is higher than the maximum possible efficiency. There exist inevitable losses when working with an actual refrigerant, ignoring any losses in the compressor. The Carnot Cycle is refrigerant independent therefore avoiding the losses associated with superheating the refrigerant.

[iv] Because of the importance of these factors, systems with a SEER of 10 can perform more efficiently than systems with a SEER of 14. The importance of these factors is frequently underestimated.

[v] This unit is among those with interesting origins. Refrigeration traditionally was accomplished through the storage and melting of ice, sometimes having salts added to encourage the highly endothermic phase change. 12,000 BTU/hr is roughly equivalent to the rate that would be provided in melting 1 ton of ice in 24 hours.

[vi] Condensate is an additional output from the system, but because of the low enthalpy and low mass flow of this stream it was neglected.

[vii] Because heat flow is typically measured in BTU/hr and electrical work in kW, this ratio will actually give the energy efficiency ratio (EER). Dividing this ratio by 3.413 BTU/kWh will give the actual value of the COP.

[viii] The heat strips for System A are not operated automatically. The controls for this backup are manual. The homeowner noted the importance of remembering to turn them off!

[ix] It is worth mentioning that a quick look at the coefficient of performance calculations shows that the COP of a heat pump operating in the heating cycle should be exactly one greater than the same pump operating in the cooling cycle. The reason this graph does not show that is because, although System A heating uses the same pump as System A cooling, it is not operating between the same temperature reservoirs. This is the reason that COP_{HP} is not equal to $COP_R + 1$.

[x] This difference is evident in the drilling of boreholes, as sedimentary wells require a casing to prevent having the well fill with sediment, whereas wells drilled into igneous and metamorphic rock do not require the same structural support.

[xi] Interestingly, and likely not coincidentally, the factor for hydraulic conductivity is also represented by the variable k. Darcy's Law is elegantly similar to Fourier's.

Darcy's Law: $Z = -KA\frac{dh}{dx}$ where Z = fluid flow, K = hydraulic conductivity of the material through which the fluid flows, A = the cross sectional area through which the fluid flows, and $\frac{dh}{dx}$ is the pressure rise (or drop, depending on the chosen convention) across the material. Similarly,

Fourier's Law: $Q = -kA\frac{dT}{dx}$ where Q = heat flow, k = thermal conductivity of the material through which the heat flows, A = the cross sectional area through which the heat flows, and $\frac{dT}{dx}$ is the temperature rise (or drop) across the material.

[xii] In fact, this portion is infinitely larger.